This article is a *Plant Cell* Advance Online Publication. The date of its first appearance online is the official date of publication. The article has been edited and the authors have corrected proofs, but minor changes could be made before the final version is published. Posting this version online reduces the time to publication by several weeks.

SWP73 Subunits of Arabidopsis SWI/SNF Chromatin Remodeling Complexes Play Distinct Roles in Leaf and Flower Development

Sebastian P. Sacharowski,[a] Dominika M. Gratkowska,[a] Elzbieta A. Sarnowska,[b] Paulina Kondrak,[a,c] Iga Jancewicz,[a,c] Aimone Porri,[d] Ernest Bucior,[a,e] Anna T. Rolicka,[a,e] Rainer Franzen,[d] Justyna Kowalczyk,[a] Katarzyna Pawlikowska,[a] Bruno Huettel,[f] Stefano Torti,[d] Elmon Schmelzer,[d] George Coupland,[d] Andrzej Jerzmanowski,[a,e] Csaba Koncz,[d,g] and Tomasz J. Sarnowski[a,1]

[a] Institute of Biochemistry and Biophysics PAS, Department of Protein Biosynthesis, 02-106 Warsaw, Poland
[b] Marie Curie Memorial Cancer Center, 02-781 Warsaw, Poland
[c] Warsaw University of Life Sciences, 02-787 Warsaw, Poland
[d] Max-Planck Institut für Pflanzenzüchtungsforschung, D-50829 Köln, Germany
[e] Universtity of Warsaw, Faculty of Biology, Institute of Experimental Plant Biology, Department of Plant Molecular Biology, 02-106 Warsaw, Poland
[f] Max Planck Genome Centre Cologne, D-50820 Köln, Germany
[g] Institute of Plant Biology, Biological Research Center of Hungarian Academy, H-6724 Szeged, Hungary

ORCID ID: 0000-0002-3805-2039 (T.J.S.)

Arabidopsis thaliana **SWP73A and SWP73B are homologs of mammalian BRAHMA-associated factors (BAF60s) that tether SWITCH/SUCROSE NONFERMENTING chromatin remodeling complexes to transcription factors of genes regulating various cell differentiation pathways. Here, we show that *Arabidopsis thaliana* SWP73s modulate several important developmental pathways. While undergoing normal vegetative development, *swp73a* mutants display reduced expression of *FLOWERING LOCUS C* and early flowering in short days. By contrast, *swp73b* mutants are characterized by retarded growth, severe defects in leaf and flower development, delayed flowering, and male sterility. MNase-Seq, transcript profiling, and ChIP-Seq studies demonstrate that SWP73B binds the promoters of *ASYMMETRIC LEAVES1* and *2*, *KANADI1* and *3*, and *YABBY2*, *3*, and *5* genes, which regulate leaf development and show coordinately altered transcription in *swp73b* plants. Lack of SWP73B alters the expression patterns of *APETALA1*, *APETALA3*, and the MADS box gene *AGL24*, whereas other floral organ identity genes show reduced expression correlating with defects in flower development. Consistently, SWP73B binds to the promoter regions of *APETALA1* and *3*, *SEPALLATA3*, *LEAFY*, *UNUSUAL FLORAL ORGANS*, *TERMINAL FLOWER1*, *AGAMOUS-LIKE24*, and *SUPPRESSOR OF CONSTANS OVEREXPRESSION1* genes, and the *swp73b* mutation alters nucleosome occupancy on most of these loci. In conclusion, SWP73B acts as important modulator of major developmental pathways, while SWP73A functions in flowering time control.**

INTRODUCTION

SWP73 (BAF60 in humans) represents an important class of accessory subunits of SWI/SNF (SWITCH/SUCROSE NONFERMENTING) ATP-dependent chromatin remodeling complexes. SWI/SNF, consisting of an SNF2 ATPase, two SWI3s, and an SNF5 subunit, is capable of nucleosome disruption through facilitation of reversible transition between normal (inaccessible) and altered (more accessible) conformations (Narlikar et al., 2002). In *Arabidopsis thaliana*, SWI/SNF complexes are involved in modulating various developmental and regulatory processes, including both vegetative and generative development, flowering time, and hormonal signaling (Sarnowski et al., 2005; Bezhani et al., 2007; Han et al., 2012; Archacki et al., 2013; Efroni et al., 2013; Sarnowska et al., 2013; Vercruyssen et al., 2014).

The enormous functional versatility of SWI/SNF complexes results from their ability to associate with diverse arrays of accessory subunits, often occurring as alternative variants. In yeast (*Saccharomyces cerevisiae*), the SWP73 protein is obligatory during growth at elevated temperature (Cairns et al., 1996). In mammals, selective incorporation of three BAF60 variants into SWI/SNF complexes directs lineage-specific cell differentiation, which is the best documented in muscle differentiation. In undifferentiated myoblasts, BAF60c is associated with the myogenic regulator basic helix-loop-helix transcription factor MyoD, an early marker of myogenic commitment. The BAF60c-MyoD complex is identified in chromatin regions of MyoD target genes, and genetic studies indicate that BAF60c enables MyoD to access its target sites in repressive chromatin of undifferentiated myoblasts. Next, likely an extracellular differentiation stimulus triggers the recruitment of catalytic and core subunits of SWI/SNF to the BAF60c-MyoD "pioneer complex," stimulating

[1] Address correspondence to tsarn@ibb.waw.pl.
The author responsible for distribution of materials integral to the findings presented in this article in accordance with the policy described in the Instructions for Authors (www.plantcell.org) is: Sebastian P. Sacharowski (sebastian.sacharowski@gmail.com).
www.plantcell.org/cgi/doi/10.1105/tpc.15.00233

nucleosome remodeling (Albini et al., 2013), which is, in turn, dependent on phosphorylation of the BAF60c Thr-229 residue by the differentiation-activated p38α kinase (Forcales et al., 2012).

Arabidopsis has two SWP73A (AT3G01890) and SWP73B (AT5G14170; also known as BAF60 or CHC1) variants. Expression of *SWP73B* responds to UV-B treatment (Campi et al., 2012) and its RNA interference (RNAi) silencing results in dwarfism (Crane and Gelvin, 2007). SWP73B was identified as an interacting partner of cyclin-dependent kinase inhibitor KRP5 (KIP-RELATED PROTEIN5), suggesting a role in controlling the cell cycle and endoreduplication (Jégu et al., 2013). Association of SWI/SNF subunits SWI3C, SWI3D, and SWP73B with ANGUSTIFOLIA3 (AN3), recruitment of SWP73B to promoters of AN3-regulated target genes *GROWTH-REGULATING FACTOR3* (*GRF3*), *GRF5*, *HECATE1* (*HEC1*), *CONSTANS-LIKE5* (*COL5*), *CYTOKININ RESPONSE FACTOR2* (*CRF2*), and *RESPONSE REGULATOR4*, and altered expression of these genes in the *brahma* (*brm*) SNF2-ATPase mutant suggest an important role of SWI/SNF complexes in the regulation of leaf development (Vercruyssen et al., 2014). Another major role of SWI/SNF complexes in flowering time control is indicated by the recent finding that SWP73B (BAF60) is involved in chromatin loop formation of the flowering time repressor *FLOWERING LOCUS C* (*FLC*) gene (Jégu et al., 2014).

In this work, we compare the regulatory functions of Arabidopsis SWP73A and SWP73B variants by correcting some misleading data derived from previously published studies of their insertion mutant alleles. Our results demonstrate that SWP73B is an important coordinator of leaf and flower development, which is involved in direct transcriptional control of key genes regulating these processes. By contrast, the function of SWP73A is confined to modulation of flowering time in short days. Further analysis of dosage-dependent effects of loss of *SWP73A* function in homozygous *swp73b* background indicates a functional overlap between SWP73A and SWP73B during embryogenesis. These findings illustrate a differential contribution of SWP73A- and SWP73B-containing SWI/SNF complexes to the regulation of transcription networks directing Arabidopsis development.

RESULTS

Interaction of SWP73A and SWP73B with Core SWI3 Subunits of Arabidopsis SWI/SNF Complexes

In animals, the number of SWP73/BAF60 variants ranges from one in *Drosophila melanogaster* to three in humans. Among plants, rice (*Oryza sativa*) and maize (*Zea mays*) have one SWP73 variant, while Arabidopsis has two, which suggests a possible functional diversification of this protein in dicots compared with monocots (Supplemental Figure 1A and Supplemental File 1). Arabidopsis SWP73s were recently confirmed to copurify with core subunits of the SWI/SNF complex (Vercruyssen et al., 2014). We used yeast two-hybrid and bimolecular fluorescence complementation (BiFC) assays to analyze the interactions of SWP73A and SWP73B variants with core components of SWI/SNF complexes including SWI3A, SWI3B, SWI3C, SWI3D, and BUSHY (BSH) (Figure 1). In these assays, SWP73A interacted only with SWI3C, whereas SWP73B could bind to both SWI3C and SWI3D (Figures 1A and 1B). Together with previous observations (Sarnowski et al., 2002, 2005; Vercruyssen et al., 2014), this suggests that SWP73 variants are incorporated into SWI/SNF complexes through their interactions with SWI3C and SWI3D (Figure 1C).

Expression patterns of *SWP73A* and *SWP73B* summarized in public transcript profiling databases show great similarity during development in different organs. Both genes are expressed in embryos, shoot and root apical meristems, leaves, and flowers (Supplemental Figures 2A to 2C). However, transcript levels of *SWP73A* are lower compared with *SWP73B* in all plant organs. Expression of *SWP73A* is upregulated in seeds and embryos passing the torpedo stage, cotyledons, and anthers during pollen formation, whereas the *SWP73B* transcript accumulates at high levels in shoot apical meristems and various flower organs.

Identification of *swp73a* and *swp73b* Insertion Mutants

We have identified two *swp73a* mutations in the JIC transposon and SALK T-DNA insertion mutant collections. The *swp73a-1* mutant allele (JIC SM_3_30546; TAIR CS117257) carried an *Spm* insertion with a duplication of GCTAC footprint at the flanks in the first exon. In the *swp73a-2* allele (SALK_083920), an inverted T-DNA repeat was inserted 310 bp upstream of the translational start codon in the promoter region of the *SWP73A* gene (Figure 2A). Quantitative RT-PCR (qRT-PCR) amplification of a 3′-segment of *SWP73A* transcript located downstream of the insertions showed that both mutant alleles were transcribed. Transcript level of *swp73a-1* allele, in which the *Spm* insertion interrupted the SWP73A reading frame, was 7-fold lower compared with the wild type. The T-DNA insertion in the promoter region of *swp73a-2* allele reduced the transcript level ~2-fold but still allowed the production of wild-type *SWP73A* mRNA (Figure 2B).

For studying the function of SWP73B, two RNAi silencing lines (CS30982 BAF60-1 and CS23961 BAF60-2) were previously constructed by Crane and Gelvin (2007) in the Wassilewskija background. In these lines, a reduction of *SWP73B* transcript level was reported to correlate with dwarfism and enhanced resistance to *Agrobacterium tumefaciens*-mediated root transformation (Crane and Gelvin, 2007). Recently, these lines were found to show a late flowering phenotype under inductive long-day conditions (Jégu et al., 2014). In addition, a homozygous SALK_113834 line carrying a T-DNA insertion in the *SWP73B* promoter region has been used in a study to demonstrate the involvement of SWP73B in DNA repair after UV-B treatment (Campi et al., 2012). Although this mutation was reported to reduce the *SWP73B* transcript level by 50% compared with the wild type (Campi et al., 2012), Jégu et al. (2014) found that the line has wild-type *SWP73B* mRNA levels and is therefore not suitable for genetic analysis. Intriguingly, although this SALK_113834 mutant is distributed as a homozygous line, we found that it is in fact heterozygous and segregates the *swp73b-1* T-DNA insertion allele. We confirmed that the T-DNA insertion in *swp73b-1* was located in the first intron interrupting

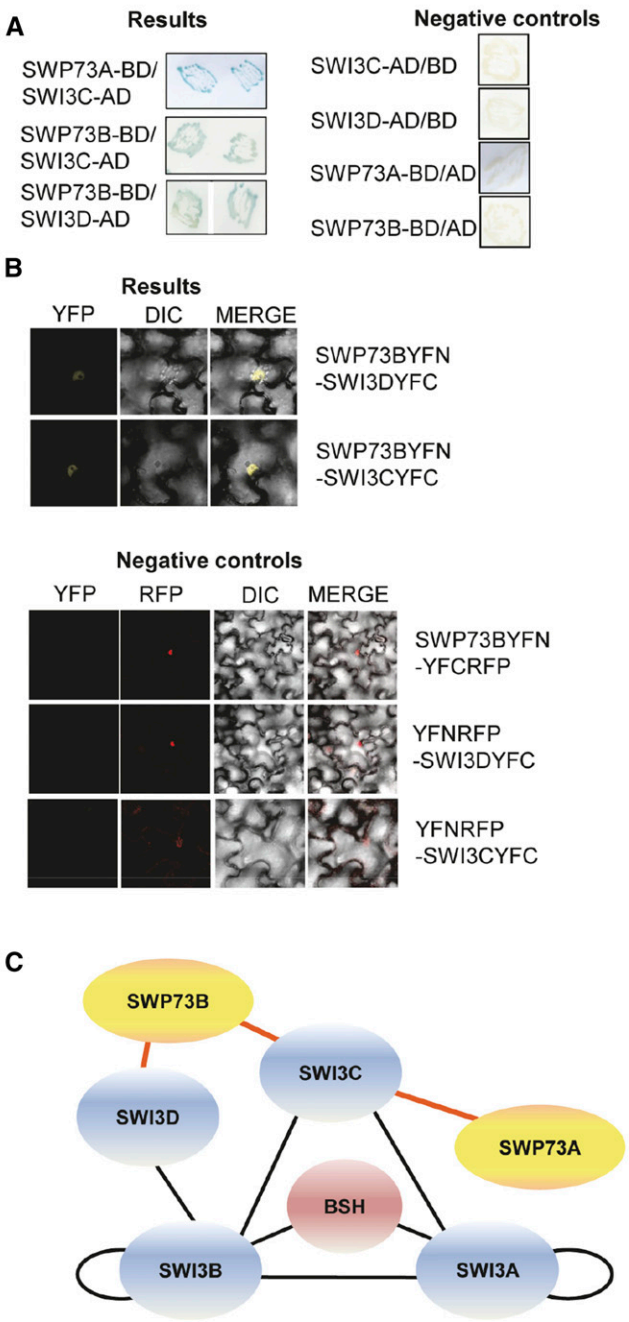

Figure 1. Arabidopsis SWP73A and B Interact with Core SWI3 Subunits of SWI/SNF Complexes.

(A) Yeast two-hybrid assays showing SWP73-SWI3 protein interactions (blue color). Right panel: controls for the yeast two-hybrid protein interaction assays.

(B) BiFC assays of in vivo interactions of SWP73B, SWI3C, and SWI3D proteins in wild tobacco (*Nicotiana benthamiana*) leaves. Left panel, YFP channel; middle panel, differential interference contrast image; right panel, merged picture. Lower panels: Negative controls for BiFC analysis including the RFP channel. Bar = 10 µm.

(C) Model of interaction network between SWP73A, SWP73B, and core subunits of SWI/SNF complex. Red lines indicate data presented in this article. Black lines indicate previously published data (Sarnowski et al., 2005; Vercruyssen et al., 2014).

the 5′-untranslated mRNA leader region. qRT-PCR analysis of a 3′ segment of *SWP73B* located downstream of insertion indicated that the transcript level was ~3% compared with the wild type in the homozygous *swp73b-1* mutant (Figure 2B). Analogously, we examined a second mutant line *swp73b-2* (SALK_071739), which was supposed to be homozygous but was found to show normal *SWP73B* transcript levels by Jégu et al. (2014). As in the case of *swp73b-1*, the *swp73b-2* line also proved to be heterozygous and carried a T-DNA insertion in the first intron, which caused a target site deletion of 19 bp (Figure 2A). qRT-PCR measurements indicated that the *swp73b-2* mutation resulted in a 5-fold reduction of *SWP73B* mRNA level compared with the wild type (Figure 2B). The observed discrepancies thus illustrate the importance of recurrent genotyping of publicly distributed T-DNA insertion mutants. All identified homozygous lines were crossed with the wild type to remove potential unlinked mutations and isolated again in homozygous form by PCR-based segregation analysis using at least 100 F3 offspring in each case.

The *swp73a* and *swp73b* Mutations Affect Different Developmental Processes

Phenotypic characterization of homozygous lines carrying either the *swp73a-1* or *swp73a-2* allele failed to reveal any distinguishing trait compared with the wild type during germination, seedling, organ development, and detailed monitoring of leaf shape, leaf blade extension, and root elongation. By contrast, the *swp73b-1* and *swp73b-2* mutations caused comparably strong and characteristic alterations in the development of vegetative and reproductive organs. Soil-grown adult *swp73b-1* plants were drastically delayed in development and had dwarf stature (Figures 2C and 2D). The weaker *swp73b-2* allele did not display larger than 10% difference in rosette and leaf size, as well as growth rate of inflorescence stem and roots compared with *swp73b-1* (Supplemental Figures 3A and 3B). Thus, phenotypic traits of the two independent mutants were nearly identical. The life cycle of *swp73b* mutants exceeded 3 months compared with mean life span of 2 months of wild-type and *swp73a* plants (Supplemental Figure 3B). Overall height of *swp73b* plants was dramatically reduced and their rosette diameter was 2- to 3-fold smaller compared with *swp73a* and wild-type plants (Supplemental Figure 3C).

While *swp73a* leaves were indistinguishable from the wild type, *swp73b* rosette and cauline leaves showed twisting along the proximal-distal axis, resulting in a downward curvature of leaf blade toward the abaxial surface. Furthermore, *swp73b* rosette leaves had an undulating surface and their length along the major vein was 2.5-fold shorter compared with the wild type following 3 weeks of development under long-day conditions (Figures 2C and 2D; Supplemental Figures 3C to 3E). These phenotypic traits indicated that the *swp73* mutations result in the alteration of both abaxial/adaxial polarity and leaf growth rate.

Whereas *swp73a* mutants produced wild-type flowers and normal seed sets, *swp73b* flowers were highly aberrant, showing a reduced number of sepals, petals, and abnormal stamens, and they never produced seeds (Figure 2E; Supplemental

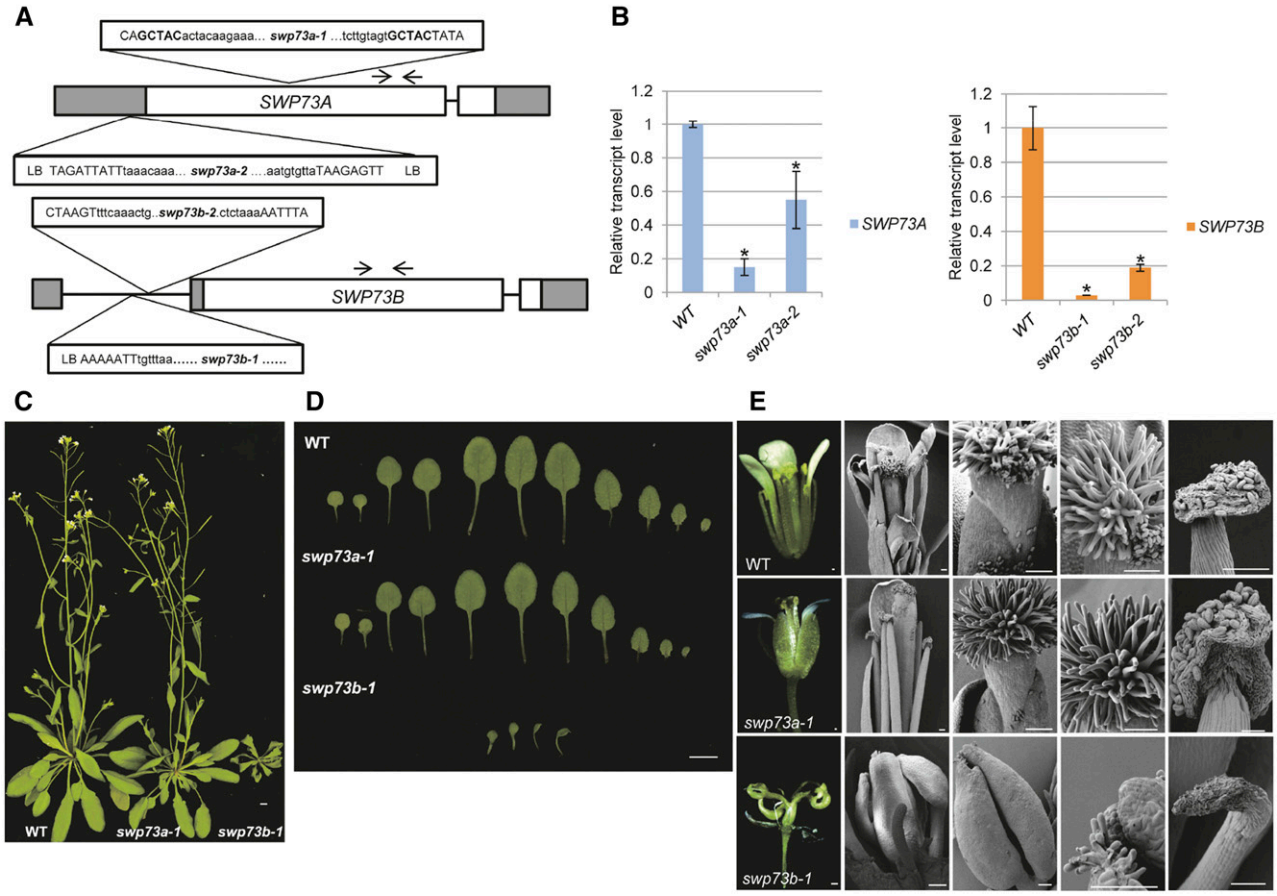

Figure 2. Characterization of *swp73a* and *swp73b* Insertion Mutants.

(A) Schematic map of position of *Spm* and T-DNA insertions in the *swp73* mutant alleles. White box, coding region; gray box, UTR; black line, intron; black arrows, primers used in qRT-PCR; uppercase letters, genome sequence; lowercase letters, insertion sequence.
(B) Transcript levels of *SWP73A* and *SWP73B* genes show a reduction in the corresponding mutant lines. Asterisks indicate significant difference from wild-type plants (error bars refer to SD, $P < 0.05$, Student's *t* test, three biological and three technical replicates were used).
(C) Five-week-old *swp73a-1*, *swp73b-1*, and wild-type plants grown in LD conditions. Note the dwarf stature of *swp73b-1* plant. Bar = 1 cm.
(D) Leaves of 15-d-old wild-type, *swp73a-1*, and *swp73b-1* plants grown in LD conditions. Note drastic developmental alteration of *swp73b-1* leaves. Bar = 1 cm.
(E) Appearance of mature flowers and analysis of their organs by scanning microscopy in wild-type, *swp73a-1*, and *swp73b-1* plants. Bar = 100 μm.

Figures 3F and 3G). In *swp73b-1* flowers, some petals were converted to sepal-like filaments. Instead of 4 and 6 in wild-type, the mean numbers of petals and stamens were 1 and 3 in *swp73b* flowers, respectively (Supplemental Figure 3F). Occasionally (in ~40% of flowers), we identified fused twin stamens as described previously for the *swi3c* and *swi3d* mutants (Sarnowski et al., 2005). In all *swp73b* flowers, the stamens carried small degenerated anthers with minimal amount of pollen. The carpels were distorted and highly degenerated, and their lower section appeared as an extension of inflorescence stem as seen previously in the *swi3d* mutant (Sarnowski et al., 2005). Furthermore, the *swp73b* mutants developed strongly retarded siliques without seeds, indicating complete sterility (Supplemental Figures 3F and 3G). In summary, severe developmental defects observed in the *swp73b* mutants compared with *swp73a* lines suggested that SWP73B plays a role in multiple developmental processes and its inactivation is not compensated for by SWP73A, either due to generally lower expression level or distinct function of SWP73A compared with its paralog.

The *swp73b* Mutation Influences Positioning of Specific Nucleosomes in the Promoter Regions of Genes Involved in Leaf and Flower Development

To examine how inactivation of SWP73A and SWP73B affects nucleosome occupancy, we performed micrococcal nuclease digestion followed by deep sequencing (MNase-Seq) using chromatin samples isolated from 14-d-old *swp73a-1* and *swp73b-1* mutant and wild-type seedlings grown under long-day conditions. During MNase digestion, the positioned nucleosomes usually protect ~150 bp of DNA. In our experiments, the average size of the nucleosome was 140 bp in each sample according to the

optimal digestion conditions described by Weiner et al. (2010). After mapping the sequence reads with Bowtie2 (Langmead et al., 2009), the data were analyzed by the DANPOS2 software using standard sample normalization options (e.g., global scaling and quantile normalization) and then Poisson tests were performed for removing background and detecting nucleosome positions (Chen et al., 2013). Compared with nucleosome occupancy on the gypsy-like transposon (AT4G07700) as a quality control (Kumar and Wigge, 2010), global distribution of nucleosome occupancy showed only minor difference in the *swp73b* mutant compared with wild-type and *swp73a* plants (Supplemental Figures 4A and 4B). The analysis of nucleosome positioning in the 5′-untranslated regions (UTRs), extending from position −3000 to the transcription start site (TSS) of each gene in the MNase-Seq data sets indicated that the *swp73a* and *swp73b* mutations resulted in nucleosome alterations in presumptive transcription regulatory regions of 4987 and 4799 genes, respectively (Supplemental Data Set 1). Alteration of nucleosome positioning occurring only in the *swp73a* or *swp73b* mutants was detected in 2157 and 1969 5′-UTRs, respectively, while 2830 5′-UTRs featured similar (2047) or different (783) changes in specific nucleosome positions in both *swp73* mutants. Gene Ontology (GO) term analysis of the *swp73*-specific MNase-Seq data set indicated an enrichment of terms related to broad classes of regulation of cellular, RNA metabolic, transcription, and RNA biosynthetic processes. In correlation with severe developmental defects detected in the *swp73b* mutants, the *swp73b*-specific data set showed an enrichment of GO terms related to developmental processes, including specific subclasses of postembryonic, reproductive shoot, and flower development (Supplemental Data Set 1). Analogously, the overlap between *swp73a* and *swp73b* data sets, in particular the subclass showing differences in nucleosome positioning between the *swp73a* and *swp73b* mutants, displayed an enrichment of GO terms related to developmental processes. As indicated by the enriched GO terms, the *swp73b*-specific MNase-Seq data set included several key genes acting in the regulation of leaf and flower development, such as *ASYMMETRIC LEAVES1* (*AS1*), *LEAFY* (*LFY*), *APETALA3* (*AP3*), *SEPALLATA3* (*SEP3*), and *AGAMOUS-LIKE24* (*AGL24*). The subclass of overlapping data, showing different nucleosome positioning in the *swp73a* and *swp73b* mutants, carried the *AS2*, *YABBY5* (*YAB5*), *AP1*, and *FLC* genes (Supplemental Data Set 1). Integrated Genome Browser view of 5′-UTRs of these genes (Figures 3A and 3B) illustrated discrete enhanced nucleosome occupancy in the *swp73b* mutant around position −1830 of the *AS1* locus (involved in the determination and maintenance of leaf polarity) upstream of a known binding site of the bromodomain-containing GENERAL TRANSCRIPTION FACTOR Group E6 (GTE6; positions −1000 to −600; Chua et al., 2005). Similarly, altered nucleosome occupancy was mapped to the −2000 to −1800 (translation start site) and −300 to −100 positions in the promoter regions of *AS2* and *YAB5* genes, respectively, which are involved in determination and maintenance of leaf polarity in Arabidopsis. Among genes involved in flowering and flower development, altered nucleosome occupancy was observed around positions 50 and −2125 to −1987 of the *AGL24* promoter (Figure 3B). The latter region contains two CArG-motifs necessary for activation of *AGL24* transcription by MADS box protein SOC1 (Liu et al., 2008). Furthermore, the *swp73b-1* mutant exhibited nucleosome stabilization and altered nucleosome occupancy around position −670 of the *AP1* locus, just upstream of known binding sites of transcription factors LFY, LMI2, SPL, and FT/FD (Pastore et al., 2011). In addition to altered nucleosome positioning in the region −740 to −1120, fuzzy nucleosome arrangement was suggested by the MNase-Seq data in *swp73b-1* mutant between positions −3000 and −2800 of *SEP3*, which carries the entry site of a transcription regulatory complex of MADS box proteins SEP3, AP1, AG, and FUL (Smaczniak et al., 2012). Nucleosome stabilization was detected around position −270 of the *AP3* promoter corresponding to a CArG-box motif (Tilly et al., 1998), which is also known to bind the BRM and SPLAYED (SYD) ATPase subunits of SWI/SNF complexes (Wu et al., 2012).

Correlation of MNase-Seq, Transcript Profiling, and ChIP-Seq Data

In order to determine to which extent altered nucleosome positioning correlates with transcriptional changes, we performed a transcript profiling experiment using Affymetrix ATH1 microarrays and RNA samples prepared from *swp73b-1* and wild-type seedlings grown under long-day conditions similarly to the MNase-Seq experiment. Analysis of the transcript profiling data using the GeneSpring software identified 1114 and 726 genes showing ≥1.5- fold higher and lower transcript levels in the *swp73b* mutant compared with the wild type, respectively (Supplemental Figure 5A). The list of genes downregulated in *swp73b* showed an enrichment of GO terms of tissue development, developmental processes, anatomical structure, and organ development following some more general terms, such as cell wall organization, responses to stimulus (hormone, organic substance, and chemicals) and biological regulation. From the downregulated genes, only 183 (25%) were found to show altered nucleosome occupancy in *swp73b* and this shared subset of genes featured similar GO terms as seen for all *swp73b* downregulated genes. Twenty of the 183 genes were GO classified to be involved in tissue development, including *KANADI3* (*KAN3*), *YAB5*, and *AGL24*, which act in leaf and flower development (Supplemental Data Set 1). GO analysis of 1114 genes upregulated in the *swp73b* mutant revealed a remarkable enrichment of terms related to biotic stress defense and cell death pathways. This suggested that parallel to the observed developmental defects, the *swp73b* mutation alters global regulation of pathogen defense responses. As seen for the downregulated gene set, only ~18% (207) of *swp73b*-upregulated genes were identified to carry altered nucleosome arrangement in their 5′-UTRs (Supplemental Figure 5B and Supplemental Data Set 1). Consequently, we concluded that only some of the transcriptional changes observed in the *swp73b* mutant can be linked to altered nucleosome arrangement. In accordance with known regulatory features of SWP73B homologs in Drosophila and mammals (e.g., Albini et al., 2013), this suggested that Arabidopsis SWP73B might also play a role in recruitment of regulatory factors prior to promoter binding of their SWI/SNF complexes. Furthermore, the small overlap between the MNase-Seq and transcript profiling data set indicated that detection of changes in nucleosome arrangement might not necessarily reflect

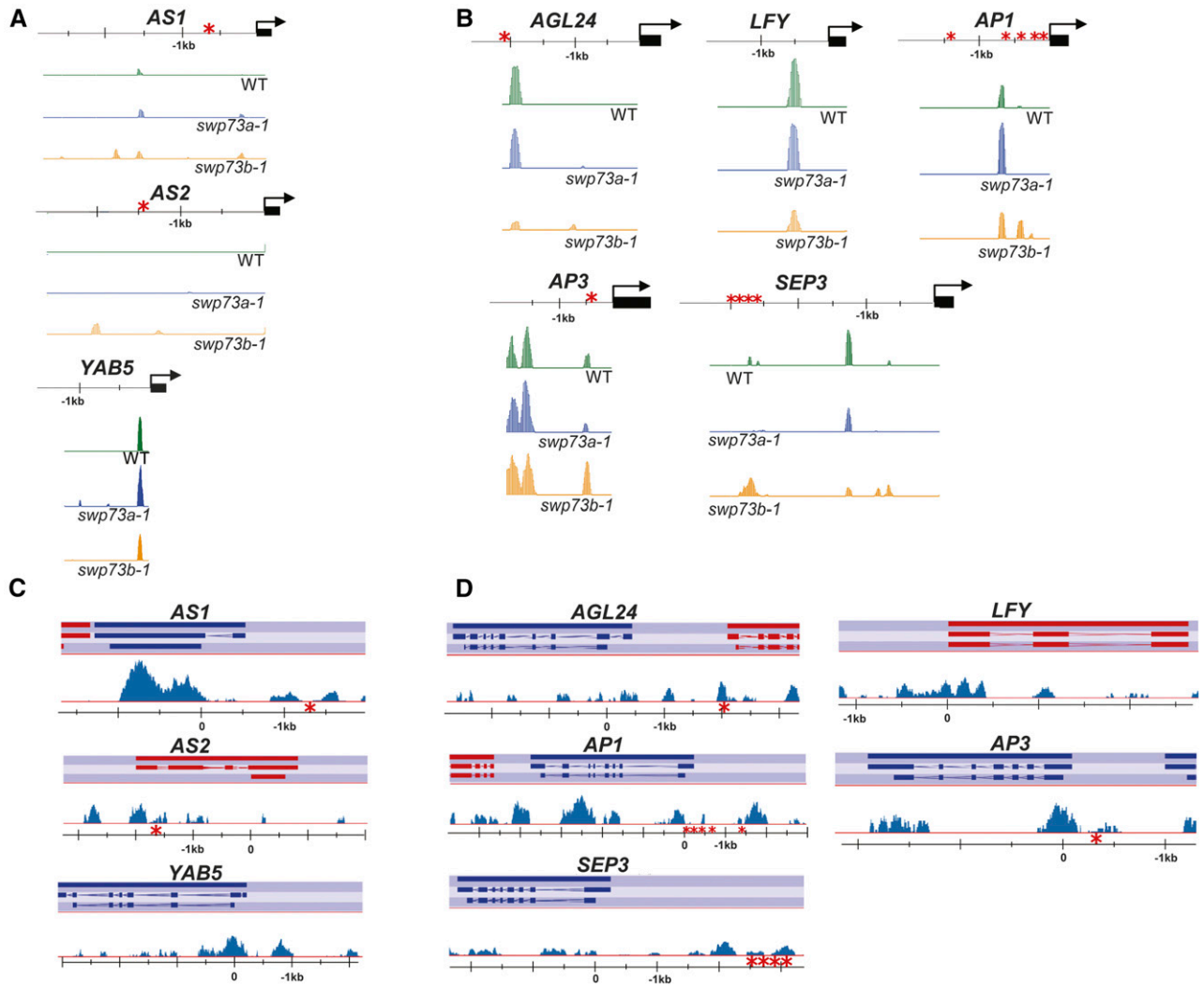

Figure 3. SWP73B-Containing SWI/SNF Complexes Determine Specific Nucleosome Positioning in Promoter Regions of Genes Involved in Leaf and Flower Development.

(A) Nucleosome distribution patterns detected by MNase-Seq analysis at the promoter regions of *AS1*, *AS2*, and *YAB5* genes influencing leaf development in 2-week-old wild-type, *swp73a-1*, and *swp73b-1* plants.
(B) Nucleosome distribution patterns observed by MNase-Seq analysis in the promoter regions of *AGL24*, *LFY*, *AP1*, *AP3*, and *SEP3* genes of flower developmental pathway in 2-week-old wild-type, *swp73a-1*, and *swp73b-1* plants.
(C) Genome browser view of SWP73B ChIP-Seq enrichment peaks in the *AS1*, *AS2*, and *YAB5* loci of wild-type and SWP73B-YFPHA plants.
(D) Genome browser view of ChIP-Seq peaks of SWP73B in the *AGL24*, *LFY*, *AP1*, *AP3*, and *SEP3* loci of wild-type and SWP73B-YFPHA plants.
Asterisks indicate known target sites of transcription factors that regulate the expression of studied loci (for more information, see description in the text).

corresponding changes of transcript levels but could also correlate with other events, such as altered transcription factor binding, chromatin loop formation, histone modifications, RNA polymerase II pausing, etc. (e.g., Lake et al., 2014).

Therefore, next we asked the question how the actual presence of SWP73B in promoter regions monitored by chromatin cross-linking and sequencing (ChIP-Seq) correlates with the MNase-Seq and transcript profiling data. As *SWP73B* showed abundant expression in all plant organs, we used a CaMV35S promoter-driven construct to genetically complement the *swp73b-1* mutation by expressing a modified SWP73B-YFP-HA protein carrying C-terminal yellow fluorescent protein (YFP) and hemagglutinin peptide epitope tags. All 20 genetically complemented lines examined were indistinguishable from the wild type (Supplemental Figure 6), indicating that this construct restored the observed developmental defects of *swp73b-1* mutant. Chromatin cross-linking and immunoprecipitation of SWP73B-YFP-HA was performed with nuclei isolated from genetically

complemented 14-d-old seedlings followed by high-throughput sequencing. Confirming an established role of SWI/SNF complexes in catalyzing chromatin remodeling throughout the gene body during transcription, discrete peaks of SWP73B enrichment were identified by analyzing the ChIP-Seq data on promoter, coding, and 3′-UTRs of transcribed Arabidopsis genes (Supplemental Figures 7A and 7B).

Subsequent comparative analysis of ChIP-Seq, MNase-Seq, and transcript profiling data identified 199 upregulated and 178 downregulated genes, which were directly targeted by SWP73B and showed altered nucleosome occupancy in the *swp73b-1* mutant. The shared downregulated ChIP-Seq and MNase-Seq data set included the *AP1*, *AGL24*, *SEP3*, *KAN3*, and *YAB5* genes (Supplemental Data Set 1). In addition to promoter regions showing altered nucleosome occupancy in our MNase-Seq study, the ChIP-Seq data also identified characteristic peaks of SWP73B representation in the coding sequences and 3′-UTRs of the *AS1*, *AS2*, and *YAB5*, as well as *AGL24*, *LFY*, *AP1*, *AP3*, and *SEP3* genes involved in leaf and flower development, suggesting an overall role of SWP73B-containing SWI/SNF complexes in their transcription (Figures 3C and 3D; Supplemental Figures 7C and 7D). In the shared upregulated ChIP-Seq and MNase-Seq data set, we identified the *FLC* gene, in which peaks of SWP73B occupancy were also detected in both 5′- and 3′-UTRs, confirming previous data on the location of SWP73B target sites in this locus (Jégu et al., 2014; Supplemental Figures 7C and 7D). In summary, our comparative transcript profiling and MNase-Seq and ChIP-Seq studies consistently identified a small set of genes that are known regulators of leaf and flower development and show association with SWP73B, in addition to altered nucleosome occupancy in the 5′-UTRs and altered transcript levels in the *swp73b* mutant. Therefore, next, we undertook a systematic confirmatory study to gain more inside into the details of how the *swp73b* mutation affects these developmental pathways.

SWP73B Plays an Important Role in Leaf Development

Recently, Vercruyssen et al. (2014) reported that the SWP73 subunits of SWI/SNF complexes interact with the AN3/GRF1-INTERACTING FACTOR1 (GIF1) transcriptional coactivator controlling cell division in leaves. The same authors found that SWI/SNF subunits SWI3C and SWP73B, as well as the SNF2-like ATPases SYD and BRM are associated with AN3 and identified BRM, SWP73A, and SWP73B in purified SWI3C complexes. Consequently, our observation that the *swp73b* mutation causes a severe defect of leaf developmental program suggested that inactivation of SWP73B inhibits the recruitment of AN3-associated SWI/SNF complexes to growth- and cell cycle-related AN3 target genes, such as *GRF5*, *GRF6*, *CRF2*, *COL5*, and *HEC1* (Vercruyssen et al., 2014). Except *GRF5*, in fact we observed that transcript levels of AN3-induced *GRF1*, *GRF4*, *HEC1*, and *COL5* genes were reduced by 40 to 60% compared with the wild type in rosette leaves of the *swp73b-1* mutant (Supplemental Figure 8A). The same AN3-induced target genes showed also somewhat lower, but significant, reduction of mRNA levels in the *swp73a-1* mutant, which supported the data of Vercruyssen et al. (2014), suggesting potential involvement of SWP73A in AN3-mediated transcription activation. However, the observed inhibition of AN3-stimulated target genes did not correlate with a growth reduction of *swp73a* mutant leaves that were indistinguishable from the wild type. Therefore, it was apparent that the *swp73b* mutation had to also affect other regulatory circuits causing major changes in leaf polarity and growth rate.

Largely distorted shape of *swp73b* leaves indicated major changes in leaf anatomy (Figure 2D). Comparative scanning electron microscopy study of leaf ultrastructure revealed greatly reduced number of palisade mesophyll cells in *swp73b-1* compared with wild-type and *swp73a-1* leaves (Figure 4A), indicating a change in specification of abaxial/adaxial cell layers. In Arabidopsis, KAN1, AS1, and AS2 are major determinants of abaxial (lower) and adaxial (upper) cell fates. We observed that transcript levels of *KAN1*, *AS1*, and *AS2* were simultaneously increased 1.8- to 2.0-fold in *swp73b* leaves compared with the wild type (Figure 4B). As *KAN1* is a transcription repressor of *AS2* and vice versa (Wu et al., 2008), this observation indicated that both abaxial and adaxial repressor activities were probably compromised in the *swp73b* mutant. Elevated KAN1 levels are known to result in feedback inhibition of *KAN2*, *KAN3*, and *YAB5*, which are involved in abaxial cell fate specification (Merelo et al., 2013; Huang et al., 2014). Accordingly, we found that transcript levels of *KAN3*, *YAB2*, *YAB3*, and *YAB5* genes showed 2- to 10-fold reduction in *swp73b* rosette leaves correlating with their highly adaxialized downward curling phenotype (Figure 4B). In comparison, *KAN1* mRNA level was only slightly increased in the *swp73a-1* mutant, which showed a parallel marginal decrease in *KAN3* mRNA level but no alteration in other *AS*, *KAN*, and *YAB* transcripts levels. In conclusion, the observed changes in *AS*, *KAN*, and *YAB* transcript levels and nucleosome occupancy detected by MNase-Seq in the promoters of *AS1*, *AS2*, and *YAB5*, as well as detection of SWP73B by ChIP-Seq analysis in the chromatin of *KAN1*, *KAN3*, *YAB2*, and *YAB3* genes suggested that SWP73B could directly participate in the regulation of their transcription. To confirm this, qRT-PCR studies were performed with cross-linked chromatin following immunoprecipitation of SWP73B-YFP-HA protein from nuclear extract of genetically complemented *swp73b-1* mutant using GFP-Trap beads and primers for amplification of promoter sequences of *AS1*, *AS2*, *KAN1*, *KAN3*, *YAB2*, *YAB3*, and *YAB5* genes. The chromatin immunoprecipitation-quantitative PCR (ChIP-qPCR) analysis indicated that cross-linked SWP73B was mapped to sequences around promoter positions −1350 of *AS1*, −2750, −1850, and −1400 of *AS2*, −1500 of *KAN1*, −1400 of *KAN3*, −650 of *YAB2*, −1750 of *YAB3*, and −1200 of *YAB5* upstream of the translation start sites (Figure 4C; Supplemental Figures 7B and 7C).

SWP73A and SWP73B Play Distinct Roles in Flowering Time Control

We observed that the *swp73b* mutant failed to flower in short-day (SD) conditions (Figure 5A; Supplemental Figure 9A). This indicated that similarly to the BRM, SYD, and SWI3 subunits of SWI/SNF complexes (Sarnowski et al., 2005; Bezhani et al., 2007; Archacki et al., 2009), their associated SWP73 factors are likely involved in the control of vegetative-to-generative phase

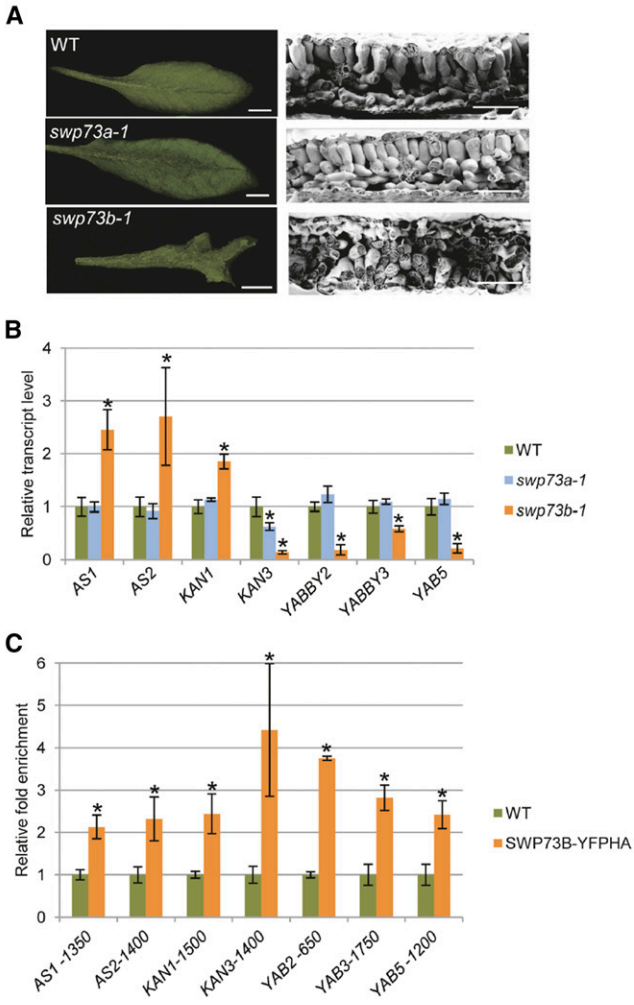

Figure 4. SWP73B Is Involved in Leaf Development.

(A) Leaves of 7-week-old wild-type and *swp73a* plants show normal development, while the *swp73b* mutant exhibits severe defect of leaf development, including a great reduction of palisade parenchyma layer. Bars = 1 cm (left panel) and 1 mm (right panel).

(B) Comparison of expression levels of genes involved in leaf development in 21-d-old wild-type, *swp73a-1*, and *swp73b-1* plants. Asterisks indicate significant differences from wild-type plants (error bars refer to SD, $P < 0.05$, Student's *t* test, three biological and three technical replicates were used).

(C) ChIP-qPCR analysis of SWP73B cross-linked promoter regions of *AS1*, *AS2*, *KAN1*, *KAN3*, *YAB2*, *YAB3*, and *YAB5* in wild-type and SWP73B-YFPHA plants using the *TA3* retrotransposon (AT1G37113) as reference. Asterisks indicate significant differences from wild-type plants (error bars refer to SD, $P < 0.05$, Student's *t* test, three biological and three technical replicates were used).

transition and/or regulation of floral homeotic genes. In fact, analogously to BRM, which was found to control the transcription of flowering time repressor *FLC* (Farrona et al., 2011), Jégu et al. (2014) reported recently that SWP73B modulates chromatin loop formation at the *FLC* locus.

Comparative analysis of *swp73a* and *swp73b* mutants revealed that the *swp73a* mutant flowered around day 23 after sowing with a mean leaf number of 13 under inductive long-day (LD) conditions similarly to the wild type. By contrast, *swp73b* flowered in LD at day 38 with a mean leaf number of 14 due to severe retardation of its development (Supplemental Figure 9A). Under noninductive SD conditions, *swp73a* plants initiated flowering with a mean leaf number of 41, significantly earlier than wild-type plants, which carried 52 leaves on average at the onset of flowering (Figure 5A; Supplemental Figure 9A). As mentioned above, the *swp73b* mutants completed their SD life cycle by decaying without flowering.

In 4-week-old SD-grown *swp73a-1* mutant, the transcript level of *FLC* was ~3-fold lower, whereas expression of *FLOWERING LOCUS T* (*FT*) was 2-fold higher compared with the wild type, consistently with its early flowering phenotype (Figure 5B). At this stage of development (i.e., using a sampling time at 6 h after onset of the light period), the mRNA levels of *CONSTANS* (*CO*), *SUPPRESSOR OF CO1* (*SOC1*), and *AGL24* (e.g., Lee et al., 2008) were similar in *swp73a* and the wild type, whereas transcript amount of *TFL1* (*TERMINAL FLOWER1*; a negative regulator of *FD*/*FT*-induced gene expression; Hanano and Goto, 2011) was about 2-fold lower in *swp73a* plants compared with the wild type. By contrast, in the *swp73b* mutant, a moderate (~1.8-fold) increase in *FLC* expression was observed, which was substantially less compared with the 5-fold increase reported by Jégu et al. (2014) in the BAF60/SWP73B RNAi lines under SD. Moreover, despite enhancement of *FLC* expression, the *swp73b* mutant displayed coordinate upregulation of *CO*, *FT*, and *SOC1* transcription in parallel with downregulation of *AGL24* and *TFL1* (Figure 5B). This clearly indicated that the flowering defect of *swp73b* plants could not result from altered expression of genes encoding canonical regulators of the flowering time pathway controlling *FT*. In this respect, it is notable that AGL24 is an activator of *SOC1*, while SOC1 stimulates *AGL24* and *LFY* transcription. Whereas *AGL24* is expressed at a low level in *swp73b* in SD, upregulation of *SOC1* could result from reduced expression of *TFL1*, which was reported to negatively regulate *SOC1* (Strasser et al., 2009). In any case, upregulation of *FT* (which also stimulates *LFY*) and *SOC1* (that together with LFY induces *AP1*, a class A floral organ identity gene specifying sepal and petal formation) was not sufficient for induction of flower meristem formation in the *swp73b* mutant. Therefore, we concluded that SWP73B probably plays a role downstream of FT and SOC1 in the control of flower meristem initiation.

The meristem identity genes *UNUSUAL FLORAL ORGANS* (*UFO*) and *LFY* (which play a key role in initiation of flower development and specify petal and stamen identity via activation of *AP3*), as well as *AP1* (at least 3-fold lower) and *SEP3* (at least 2-fold), showed markedly reduced transcript levels in *swp73b* compared with the wild type (Figure 5C). The *SEP1-4* genes are required for the specification of all four types of floral organs. Expression of *SEP3* is directly regulated by AP1 and several other MADS box proteins (Smaczniak et al., 2012). In comparison, the *swp73a* mutation had no significant effect on the expression of these floral organ identity genes. As observed under SD condition, the *swp73b* mutation also resulted in downregulation

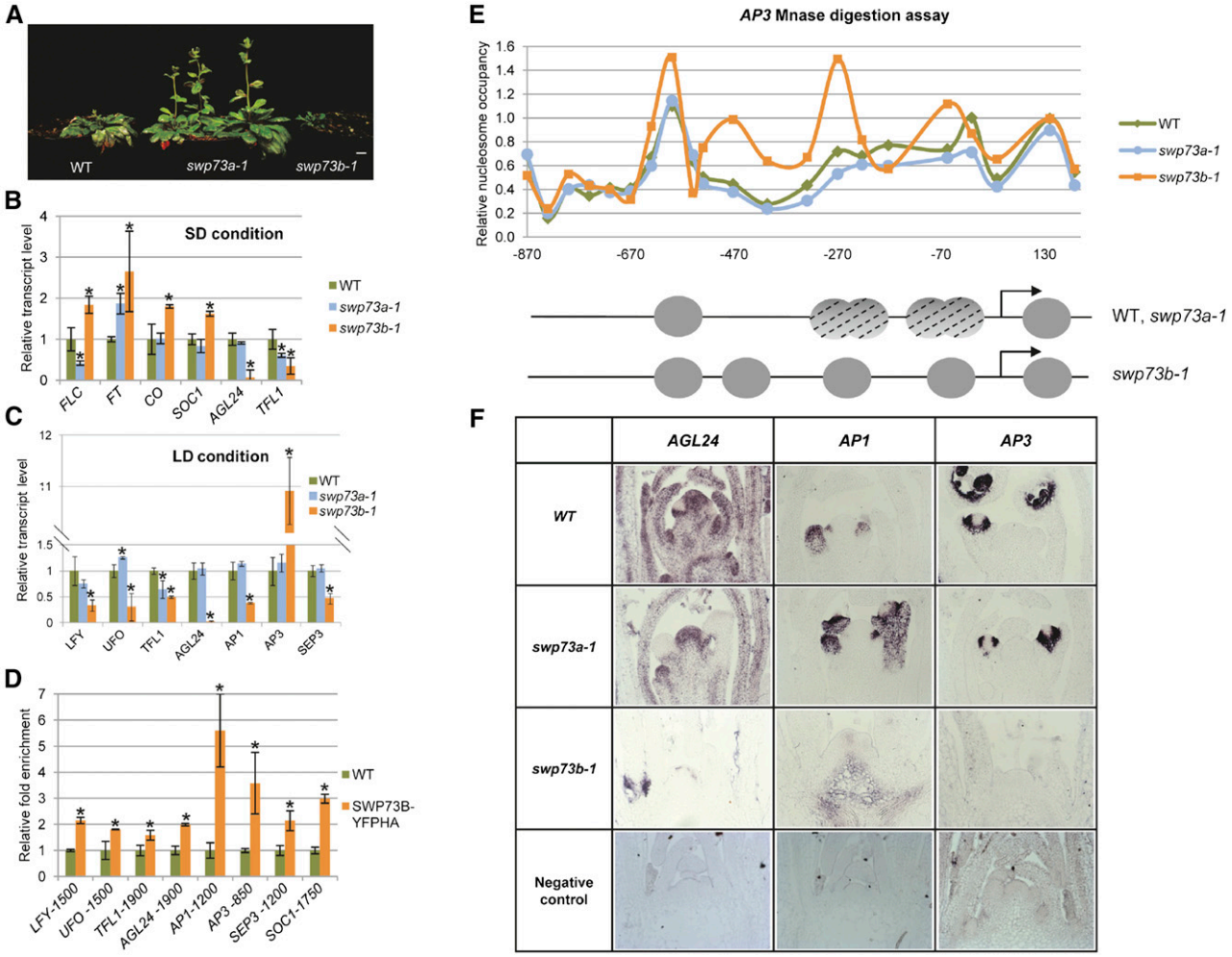

Figure 5. SWP73A and SWP73B Differently Affect Flower Development and Flowering Time Control.

(A) Comparison of 8-week-old SD-grown wild-type, *swp73a-1*, and *swp73b-1* plants. Bar = 1 cm.

(B) qRT-PCR analysis of expression of genes involved in control of flowering in 4-week-old SD-grown plants. Asterisks indicate significant differences from wild-type plants (error bars refer to SD, $P < 0.05$, Student's *t* test, three biological and three technical replicates were used).

(C) qRT-PCR analysis of expression of genes involved in the control of floral meristem identity in 2-week-old LD-grown plants. Asterisks indicate significant differences from wild-type plants (error bars refer to SD, $P < 0.05$, Student's *t* test, three biological and three technical replicates were used).

(D) ChIP-qPCR analysis of SWP73B location in the promoter regions of *LFY*, *UFO*, *TFL1*, *AGL24*, *AP1*, *AP3*, *SEP3*, and *SOC1* genes in wild-type and SWP73B-YFPHA plants using the *TA3* retrotransposon as reference. Asterisks indicate significant differences from wild-type plants (error bars refer to SD, $P < 0.05$, Student's *t* test, three biological and three technical replicates were used).

(E) Relative nucleosome occupancy of *AP3* promoter in 2-week-old wild-type, *swp73a-1*, and *swp73b-1* plants. Upper panel: Nucleosome occupancy of *AP3* promoter analyzed by MNase digestion followed by qPCR with tiled primers. The fraction of undigested genomic DNA amplified for each amplicon was normalized to that of the −73 position of gypsy-like retrotransposon (AT4G07700) as control. Lower panel: Schematic illustration of positions and dynamics of nucleosomes on the *AP3* promoter in wild-type, *swp73a-1*, and *swp73b-1* plants. Gray circles represent positioned nucleosomes, and dashed circles correspond to nucleosomes that are not positioned.

(F) In situ hybridization of antisense *AGL24*, *AP1*, and *AP3* transcripts in shoot apical meristems of 14-d-old wild-type, *swp73a-1*, and *swp73b-1* plants. Note irregular shape of *swp73b-1* meristem.

of *AGL24* and *TFL1* in LD. Intriguingly, *TFL1* also showed similarly reduced transcript levels in the *swp73a* mutant correlating with its early flowering phenotype.

Our MNase-Seq and ChIP-Seq studies indicated that SWP73B was represented in the chromatin of several genes involved in the control of flower development and that the *swp73b* mutation caused some alterations in the nucleosome occupancy of their promoter regions. Additionally, the transcript profiling data also indicated reduced expression of key genes involved in the control of flower development in the *swp73b* line. To confirm that SWP73B-containing SWI/SNF complex plays a direct role in the transcription of *LFY*, *UFO*, *TFL1*, *AGL24*, *AP1*,

AP3, *SEP3*, and *SOC1* genes, we performed a ChIP-qPCR analysis as described above using *swp73b* plants genetically complemented with the 35S promoter-driven SWP73B-YFP-HA construct. The ChIP-qPCR data indicated ~2-fold enrichment of cross-linked SWP73-YFP-HA around positions −1425 of *LFY*, −1575 of *UFO*, −1825 of *TFL1*, and −1975 of *AGL24* promoters. SWP73B showed ~5-fold enrichment at positions −1125 to −1275 of *AP1*, 4-fold enrichment at the −400 to −900 region of *AP3*, and 2- to 3-fold enrichment around positions −1125 to −1275 of *SEP3* and −1675 to −1825 of *SOC1* promoters delineating the SWP73B entry sites (Figure 5D; Supplemental Figure 9B). In the case of *AP3*, our mapping data (i.e., positions −400 to −900) perfectly matched to previously determined ChIP positions of SWI/SNF ATPase subunits SYD and BRM (Wu et al., 2012), which are located in the vicinity of CArG motifs implicated in stamen (positions −200 to −100 and −496 to −332) and petal (positions −332 to −225) development (Tilly et al., 1998). On the other hand, the cross-linked position of SWP73B was located in immediate vicinity of previously mapped binding site of SOC1 (Liu et al., 2008).

Among transcriptional changes observed in *swp73b*, the most striking event was a 10-fold activation of *AP3*, which occurred despite downregulation of the *AP3* activators LFY and UFO. This, together with qPCR confirmation of ChIP-Seq data and observed alteration of nucleosome occupancy by MNase-Seq in the *swp73b* mutant (Figure 3B), suggested that SWP73B plays a role as *AP3* repressor, while acting as positive regulator of the transcription of other floral identity genes. To strengthen this conclusion, we performed MNase protection assays with chromatin extracts isolated from wild-type, *swp73a*, and *swp73b* plants. In both wild-type and *swp73a* plants, a DNA fragment protected from MNase digestion was mapped between positions −330 and +40 of the *AP3* promoter, corresponding to two nucleosomes located immediately upstream of the transcription start site (Figure 5E; Supplemental Figure 10). The lack of clearly separated peaks (i.e., DNA fragments of ~150 bp) indicated that none of the two nucleosomes were strictly positioned. By contrast, a well-defined gap between −1 and −2 nucleosomes upstream of TSS was detected in the *swp73b-1* mutant, indicating normal (i.e., closed/inaccessible) nucleosome positioning. Furthermore, the lack of SWP73B binding to the *AP3* promoter in the *swp73b* mutant resulted in clear positioning of −3 nucleosome, which was not observed in wild-type or *swp73a* plants. Consequently, these results demonstrated that SWP73B is required for SWI/SNF chromatin remodeling activity in the promoter region of *AP3* gene. Together with observed derepression of *AP3* transcription in the *swp73b* mutant, this showed that a chromatin remodeling event is necessary for repression of *AP3* transcription. These data also explained why reduced transcription of UFO and LFY (i.e., positive regulators of *AP3*) had no apparent effect on the control of *AP3* transcription in the *swp73b* mutant. Nevertheless, overexpression of *AP3* in the *swp73b* mutant was inconsistent with the observed flower phenotype of *swp73b-1* plants. To clarify this apparent discrepancy, we performed in situ hybridization studies with meristems of LD-grown *swp73a-1*, *swp73b-1*, and wild-type plants (Figure 5F). Compared with *swp73a-1* and the wild type, the shoot meristem of the *swp73b-1* mutant featured typical vegetative stage, lacking primordia of floral buds. The *AGL24*, *AP1*, and *AP3* transcripts showed similar expression patterns in wild-type and *swp73a-1* meristems. *AGL24* expression was ubiquitous, with clear enhancement in floral bud primordia, whereas both *AP1* and *AP3* transcripts were detected only in the floral bud primordia. *AGL24* exhibited greatly reduced transcription similarly to *AP1*, which displayed ectopic expression in the basal region of *swp73b-1* mutant shoot meristem. This observation further supported the conclusion that SWP73B is required for proper maintenance of *AGL24* and *AP1* expression in the inflorescence meristem. By contrast, we detected a complete lack of *AP3* expression in *swp73b-1* meristems, which indicated that high transcript levels of *AP3* detected by qRT-PCR measurement in *swp73b-1* seedlings resulted from ectopic activation of *AP3* transcription. To unequivocally demonstrate this, *AP3* transcript levels were measured by qRT-PCR in leaves separated from meristems of 2-week-old plants. In comparison to control *swp73a-1* and wild-type plants, transcript level of *AP3* was ~13-fold higher in *swp73b-1* leaves (Supplemental Figure 11), confirming that inactivation of SWP73B leads to ectopic derepression of *AP3* in leaves.

In conclusion, the data described above revealed important functional differences between SWP73A- and SWP73B-containing SWI/SNF complexes in the regulation of flowering time and development of flower organs. SWP73A appears to exert its effect solely through controlling *FLC* expression, while SWP73B has a much wider regulatory function. Complete inability of the *swp73b* mutant to induce flowering under non-inductive SD conditions, dramatic alterations in flower organ differentiation in LD, and complete sterility of *swp73b* plants suggest a key role of SWP73B-SWI/SNF complexes in overall control of vegetative to generative phase transition, flowering time, and specification of floral organ identity. In addition, SWP73B dependence of nucleosome movements within the *AP3* promoter suggests that this particular SWP73 subunit is an important determinant of chromatin plasticity within *cis*-regulatory sequences of regulatory genes involved in these developmental processes.

Dosage-Dependent Effects of *swp73* Mutations during Embryogenesis

Our data described so far supported the conclusion that SWP73A and SWP73B perform nonoverlapping regulatory functions. Nonetheless, we could not unequivocally exclude their functional redundancy because *SWP73B* is expressed at much higher levels in most plant organs compared with *SWP73A* (Supplemental Figure 2). To address this question using genetics, we constructed reciprocal double mutants carrying one of the alleles in homozygous and the other one in heterozygous form. Briefly, upon crossing *swp73a* with *swp73b*/+, a *swp73a*/+ *swp73b*/+ line was generated by PCR-based genotyping. In addition to wild-type seeds, after self-pollination, the siliques of *swp73a*/+*swp73b*/+ plants contained 2.4% of arrested ovules and 6.3% of white translucent seeds, which degenerated into collapsed brown aborted seeds upon maturation (Figure 6A; Supplemental Figure 12A). Comparative microscopic analysis of developmental status of embryos in green wild-type and white aborted seeds 4 d after

fertilization using Nomarski optics identified embryos at heart stage in wild-type seeds, whereas all white seeds carried embryos arrested at early globular stage (Figure 6B; Supplemental Figure 12B). The frequency of segregating white seeds with arrested embryos suggested that they represent the double homozygous *swp73a swp73b* class. To verify this, we identified *swp73a swp73b*/+ lines and found that their siliques contained 7% arrested ovules, 17% white aborted, and 76% green seeds (Figure 6A; Supplemental Figure 12A). Recurrent microscopic inspection of white seeds indicated that the endosperm was not cellularized, which is a characteristic trait in early stages of seed development. Among the embryos arrested in early globular stage, we detected variants with abnormal cell shapes and division patterns in the suspensor and embryo proper, the latter showing either two-cell or quadrant stage (Figure 6B; Supplemental Figure 12B).

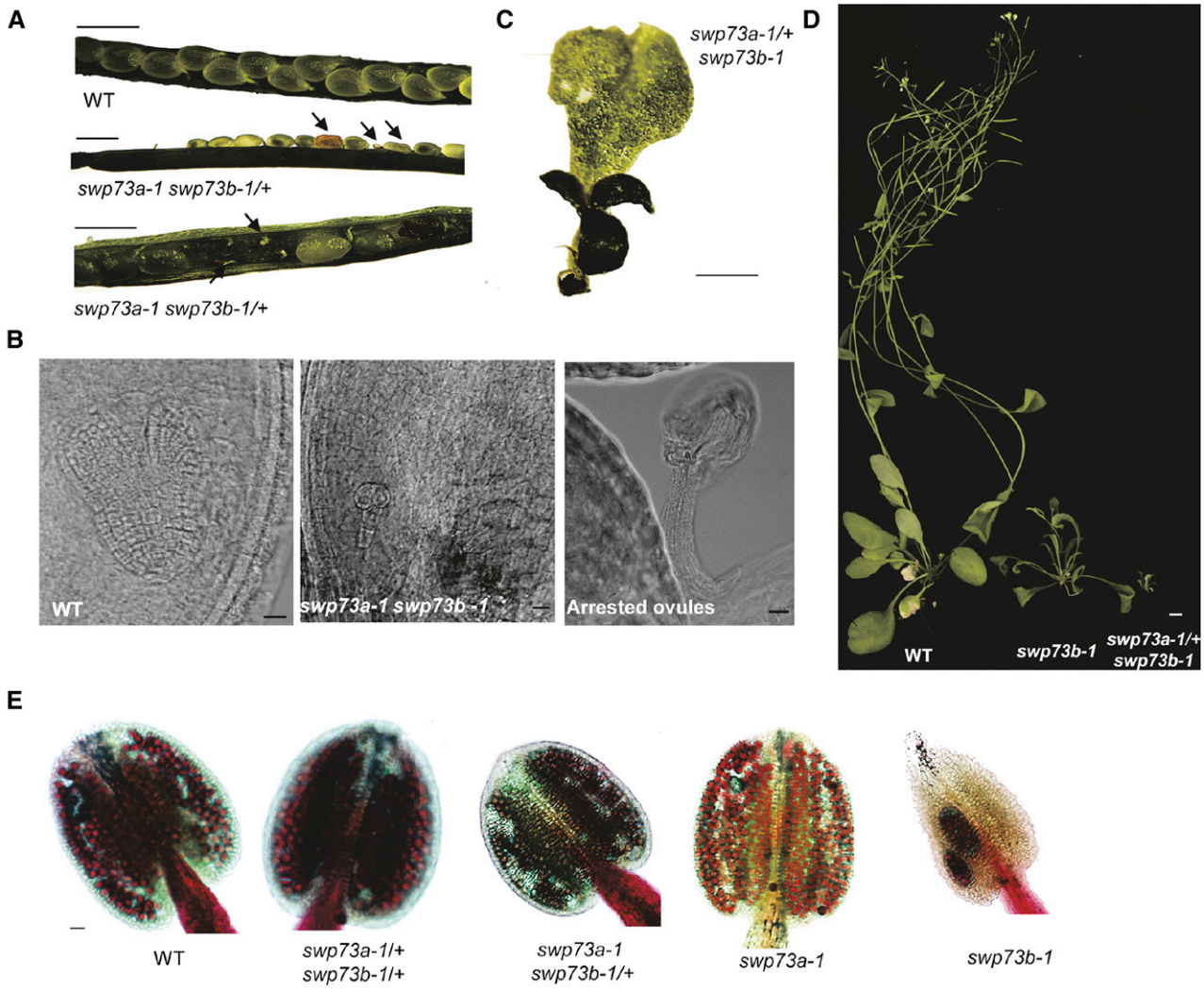

Figure 6. Effects of Concomitant Inactivation of *SWP73A* and *SWP73B* on Embryo Development.

(A) Comparison of open siliques of wild-type and *swp73a swp73b-1*/+ plants. The occurrence of white aborted seeds demonstrates embryo lethality; arrested ovules indicate female gametophyte lethality. Bar = 0.5 mm.

(B) Nomarski images of green wild-type-like and white *swp73a swp73b* seeds at the same stage of development and arrested ovules. The inspection indicated regular heart-stage embryos in wild-type-looking green seeds. White translucent seeds contained an aberrant globular-stage embryo. Bar = 10 μm.

(C) Three-weeks-old LD-grown *swp73a-1*+*swp73b-1* plants exhibit ectopically positioned meristems and aberrant shape cotyledons and leaves. Bar = 1 mm.

(D) Comparison of 4-week-old LD-grown wild-type, *swp73b-1*, and *swp73a*/+*swp73b* mutants indicates strong growth retardation of *swp73a*/+*swp73b* plants. Bar = 1 cm.

(E) Examination of pollen viability in the anthers of *swp73a-1*, *swp73b-1*, *swp73a swp73b*/+, and *swp73a*/+*swp73b*/+ lines by Alexander staining. Red staining, viable pollen grains; green staining, dead pollen grains. Bar = 10 μm.

Because reduced frequency of white aborted (*swp73a swp73b*) seeds suggested reduced transmission of the *swp73b* allele in the *swp73a* mutant background, we performed reciprocal crosses. First, *swp73a* pistils were fertilized with pollen of *swp73a swp73b*/+ plants. The F1 hybrids showed a 69:31 segregation ratio of *swp73a*: *swp73a swp73b*/+ progeny, indicating reduced male transmission of *swp73b* mutant allele. When pollinating *swp73a swp73b*/+ pistils with *swp73a* pollen, analogously we observed a segregation ratio of 65:35 for the *swp73a*: *swp73aswp73b*/+ offspring, which revealed reduced female transmission of the *swp73b* allele (Supplemental Figure 12C). Next, we performed a detailed segregation analysis of progeny of *swp73a*/+*swp73b*/+ line using both PCR genotyping and phenotypic classification (Supplemental Figure 12D). As expected, we observed a distorted Mendelian ratio of different F2 classes. The offspring carrying wild-type *SWP73B* allele (e.g., *SWP73ASWP73B*; *swp73aSWP73B* and *swp73a*/+*SWP73B*) was enriched, the representation of classes containing a single mutant *swp73b* allele was reduced, and the *swp73a*/+*swp73b* class was the most underrepresented. Compared with *swp73b*, the *swp73a*/+ *swp73b* mutants showed enhanced dwarfism (reaching to ~5-mm height by day 21 in LD conditions), altered shape of cotyledons and first true leaves, ectopically positioned meristems, and short life span (~3 weeks; Figures 6C and 6D). This indicated a clear dosage-dependent effect resulting from removal of one of the two *SWP73A* alleles in the homozygous *swp73b* background. As a confirmatory study, we next examined the pollen viability in the anthers of *swp73a-1*, *swp73b-1*, *swp73a swp73b*/+, and *swp73a*/+*swp73b*/+ lines by staining with Alexander solution (Figure 6E). Anthers of *swp73a-1* and wild-type plants produced ample red-stained viable pollen, which was also detectable in *swp73b-1* anthers but in reduced amounts. In comparison, anthers of *swp73a*/+*swp73b*/+ line contained markedly higher amounts of dead green pollen grains, which is consistent with the observation of reduced representation of *swp73a*/+*swp73b* and *swp73b* mutant classes in F2 progeny, as well as reduced male transmission of *swp73a*/+ *swp73b* gametes.

Finally, we tested whether inactivation of one of the SWP73 variants would influence the transcript level of the other allele (Supplemental Figure 12E). Remarkably, whereas the *swp73a* mutation resulted only in a marginal increase in *SWP73B* expression, the transcript level of *SWP73A* was increased 2-fold in the *swp73b* mutant, indicating the existence of an intriguing compensation mechanism. Together with the observation that the loss of one functional *SWP73A* allele in *swp73a*/+*swp73b* led to aggravated dwarfism and seedling lethality, these data indicated that a single functional *SWP73A* allele is not sufficient to compensate for the lack of SWP73B function, whereas SWP73B can fully balance inactivation of SWP73A. The enhanced growth defect of *swp73a*/+ *swp73b* plants also illustrates that the function of SWP73A becomes biologically significant only in the absence of functional SWP73B. On the other hand, female gametophyte lethality of *swp73a swp73b*/+ plants (which is not observable in the *swp73b* due to its full sterility) is consistent with a role of SWP73B in gametophyte development, which becomes observable only when SWP73A is inactivated. Finally, early embryonic lethality of the *swp73 aswp73b* double mutant indicates that at least one of the SWP73 variants is necessary for viability in Arabidopsis.

DISCUSSION

Our knowledge of the regulatory functions of plant SWI/SNF complexes was derived thus far from functional characterization of their core SWI3 and SNF2-like BRM and SYD ATPase subunits based on the identification of yeast two-hybrid and BiFC interacting partners, knockout mutations, and targeted ChIP studies with genes showing altered transcription in these mutants. The emerging data indicate that Arabidopsis SWI/SNF complexes are required for proper regulation of embryo, seed, root and flower development; flowering time; abscisic acid (ABA), gibberellin, and other hormone signaling pathways; and several basic processes, such as cell cycle progression, endoreduplication, chromatin condensation, imprinting etc. Compared with other organisms, the higher copy number of genes encoding most plant SWI/SNF subunits provides the advantage that ultimate lethality of knockout mutations is often overcome by unbalanced expression of functionally redundant subunit variants, which facilitates genetic analysis and thereby fine dissection of subunit-specific functions.

It is apparent that various SWI/SNF subunits recognize distinct regulatory partners mediating chromatin remodeling at different target loci, although the mechanisms regulating gene-specific recruitment of SWI/SNF complexes are largely elusive. Arabidopsis BRM is known to carry three putative DNA binding motives, including an AT-hook and a C-terminal bromodomain recognizing histones H3 and H4 (Farrona et al., 2007). BRM is a repressor of *FLC*, *CO*, *FT*, and *SOC1* in the flowering time pathway. The *brm* mutation enhances the level of histone H3 lysine 4 trimethylation and renders dispensable the incorporation of histone H2A.Z variant into chromatin at promoter regions of these target genes leading to their transcriptional activation (Farrona et al., 2011). BRM and SYD are reported to redundantly counteract Polycomb-mediated repression of class B and C flower homeotic genes *AP3* and *AG*, respectively, likely by interacting with their transcriptional activators LFY and SEP3 (Wu et al., 2012). BRM was also ChIP mapped to the promoter of seed storage protein gene *2S2*, which shows derepressed expression in leaves of *brm*, *swi3c*, and *bsh* mutants (Tang et al., 2008). Furthermore, BRM was shown to repress *ABSCISIC ACID INSENSITIVE5*, a key positive regulator of ABA signaling, by binding to its promoter and regulating ABA-dependent nucleosome rearrangement (Han et al., 2012). Although BRM and SYD are thought to perform partially overlapping functions, SYD interacts preferentially with the SWI3A and B core subunits, a binding partner of FCA required for FLC expression, whereas the binding partners of BRM in the SWI/SNF core are SWI3B and SWI3C (Sarnowski et al., 2002; Bezhani et al., 2007). For the majority of target genes showing altered transcription in SWI/SNF subunit mutants, the composition of SWI/SNF complexes and their interacting transcription factor partners are thus far unknown. Although the BRM and SYD ATPases appear to be involved in both nucleosomal and gene-specific targeting of SWI/SNF complexes, it is still an open question whether and how other SWI/SNF subunits participate in these processes.

In mammals, different alternative variants of SWP73/BAF60 SWI/SNF subunits have been uncovered to play major roles in tissue-specific regulation of gene expression (Takeuchi and Bruneau, 2009; Forcales et al., 2012). Detailed functional characterization of the two Arabidopsis SWP73 homologs has been so far handicapped due to lack of suitable null mutations. Using RNAi lines, it was nevertheless established that partial silencing of *SWP73B* inhibits seedling growth, leading to dwarfism, as well as cell division in Agrobacterium-transformed roots (Crane and Gelvin, 2007). Recently, Jégu et al. (2014) observed that the SWP73B RNAi lines show a weak late flowering phenotype in LD, which is due to defective formation of a repressive chromatin loop causing transcriptional activation of the flowering time repressor *FLC*. Based on a systematic proteomics approach, Vercruyssen et al. (2014) identified SWP73B as an interacting partner of AN3/GIF1, as well as SWI3C, SYD, and BRM in purified AN3 complexes, and found BRM, SWP73A, and SWP73B in SWI/SNF complexes purified by tagged SWI3C. This work also revealed that SWP73B is directly targeted to AN3-activated target genes, including GRF5, GRF6, CRF2, COL5, HEC1, and probably CYCB1;1. As the *brm* mutation greatly augmented the *an3* narrow leaf defect, it was concluded that SWI/SNF (carrying likely BRM, SWP73A or B, SWI3C and D, and possibly BSH) is required for AN3-mediated control (i.e., activation) of cell division in leaves, specifically in pavement cells around the stomata.

Here, we described the identification of thus far missing insertion mutants for both Arabidopsis *SWP73* loci, which enabled us to compare their deficiencies to those of earlier studied *brm* and *swi3* mutants (Sarnowski et al., 2005; Archacki et al., 2009, 2013; Sarnowska et al., 2013). In Arabidopsis, *SWP73A* is transcribed at much lower levels in most organs and developmental stages compared with *SWP73B*. Therefore, if the two variants were functionally redundant, it is logically expected that high expression of SWP73B will compensate for the loss of SWP73A in most pathways. In fact, plants carrying either the *swp73a-1* or *swp73a-2* mutant alleles are indistinguishable from the wild type except under SD conditions, where they flower significantly earlier correlating with a downregulation of *FLC* and concomitant induction of *FT*. Therefore, SWP73A appears to act as a positive regulator of *FLC* in SD and performs a function opposing SWP73B, which when inactivated by T-DNA insertions or silenced by RNAi prevents flowering or confers a late flowering phenotype (Jégu et al., 2014), respectively. In *swp73b* insertion mutant and RNAi silenced lines, *FLC* transcript levels are higher compared with the wild type, but *FT*, *CO*, and *SOC1* expression is also markedly induced. This suggests that the flowering defect caused by the *swp73b* mutation disrupts the pathway downstream of *FLC*, *FT*, and *SOC1*. It is notable that in *swp73b* mutants, enhanced expression of *FLC* fails to suppress *FT* and *SOC1*, whereas *AGL24* is remarkably downregulated despite higher expression of its activator SOC1, correlating with the late flowering phenotype.

In comparison to *swp73b*, the *brm*, *swi3c*, and *swi3d* mutants also show a remarkably timely delay in flowering compared with the wild type but produce a lower number of leaves in both SD and LD. Therefore, they are classified as early flowering mutants. According to Jégu et al. (2014), in the RNAi-silenced *swp73b* lines, the *FT* transcript levels are slightly higher compared with the wild type despite 4- to 5-fold increase in *FLC* expression, whereas *SOC1* is markedly downregulated in inductive LDs. Our data show that transcript levels of *AGL24* are also very low in LD. Thus, *AGL24* expression is compromised in *swp73b* independently of daylength (i.e., photoperiodic pathway) and changes in the regulation of *FLC.*

Our study indicates that SWP73B has broader and more important regulatory functions than SWP73A. The effect of *swp73a* mutation is visible only when the SWP73B subunit is not functional (i.e., heterozygous *swp73a* in background of homozygous *swp73b* or as double mutant, which is embryo lethal). Whereas the *swp73a* mutation does not alter normal differentiation of floral organs, in *swp73b* flowers, the number of sepals and petals is remarkably reduced, and sepaloid petals, twin stamens, and split carpels are formed frequently, as observed previously in the *swi3c* and *swi3d* mutants. As in the case of the flowering time pathway, it is rather difficult to identify potential floral homeotic gene targets of the SWP73B-SWI/SNF complex based solely on monitoring transcript levels in the *swp73b* mutant. Therefore, we performed global analysis of nucleosome occupancy in *swp73a* and *swp73b* to address the question about the molecular mechanism underlying the observed phenotypic changes (i.e., altered leaf and flower development). Whereas the loss of either SWP73A or SWP73B does not appear to influence global nucleosome occupancy, the MNase-Seq study followed by GO classification indicated that SWP73B is involved in the regulation of developmental processes. Closer inspection of promoter regions of *AS1*, *AS2*, and *YAB5* genes regulating leaf development, as well as *AGL24*, *LFY*, *AP1*, *AP3*, and *SEP3* acting in flower development, documents a role for SWP73B in specific regulation of nucleosome positioning. Our data demonstrate that inactivation of SWP73B alters nucleosome positioning at specific promoter positions that correspond to previously mapped regulatory regions involved in the developmental regulation of transcription of these genes. Transcript profiling study, qRT-PCR transcript measurements, MNase-Seq detection of altered nucleosome occupancy, and ChIP-Seq analysis of SWP73B chromatin representation corroborate an important role of SWP73B in the regulation of the *AS1*, *AS2*, *YAB5*, *AGL24*, *LFY*, *AP1*, *AP3*, and *SEP3* genes. At the same time, these comparative studies have shed light on several other pathways, such as the regulation of pathogenic defense responses, which are also influenced by the loss of SWP73B function and thus deserve attention in future examinations. We also noted that the ChIP-Seq data show that localization of SWP73B is not confined to promoters but shows a wider distribution in gene bodies and 3′-UTRs, as reported previously for human SWI/SNF complexes (Euskirchen et al., 2011). It thus remains a challenge to determine how the *swp73b* mutation influences overall localization of SWI/SNF complexes in different regions of gene targets at the genome-wide level.

When discussing the effects of *swp73* mutations on regulation of genes directing leaf and flower development, it is important to consider that SWP73s act as accessory subunits, the function of which reflects their interactions with other components of SWI/SNF complexes. In the regulation of chromatic remodeling, SWI/SNF complexes appear to act in concert, implying direct interaction

with Polycomb (PC) repressors. In animals, the BRM SNF2-type ATPase is thought to be the sole SWI/SNF subunit required for eviction of PC repressor from promoters (Francis et al., 2001). In this respect, it is interesting that in the pathway determining floral organ identity, UFO and LFY were reported to induce *AP3* in whorls 2 and 3 through recruitment of BRM-SWI/SNF complex through direct interaction of BRM with LFY and SEP3 at the *AP3* promoter (Liu and Mara, 2010; Wu et al., 2012). In *swp73b*, the expression of *LFY* and *UFO* is reduced, but *AP3* nevertheless shows highly elevated transcription compared with the wild type, in contrast to *brm* but similarly to the *swi3d* mutant (Sarnowski et al., 2005; Wu et al., 2012). It is thus conceivable that the SWI/SNF core carrying SWP73B, SWI3C, and SWI3D in the *brm* mutant could recruit Polycomb-2 conferring a repression of *AP3*, which is abolished by inactivation of SWP73B. Whereas BRM appears to act as an activator of *AP3*, it represses the transcription of *FLC*, *CO*, *FT*, and numerous other genes. Enhanced transcription of BRM-repressed genes in the *swp73b* mutant suggests that SWP73B might be required for SWI/SNF recruitment of BRM. In any case, based on overexpression of *AP3* in *swp73b* (and *swi3d*), one would expect a replacement of carpels by stamens, producing a *superman*-like phenotype (Jack et al., 1994). Instead, we find a reduction in the number of stamens and petals, indicating a strong inhibition of the *AP3*-dependent male specification program. Our in situ hybridization studies show that *AP3* is not expressed in the shoot meristem but rather shows ectopic derepression in leaves. This suggests that SWP73B plays a pivotal role in repressing *AP3* expression in vegetative tissues, probably independently of BRM. By contrast, SWP73B is required for proper maintenance of *AGL24* and *AP1* expression, as well as other floral organ identity genes in the floral meristem. This conclusion is strongly supported by our ChIP mapping data, which show that cross-linked SWP73B and regions of altered nucleosome occupancy in the *swp73b* mutant either overlap or are located in the vicinity of promoter sequences that represent known binding sites for MADS domain transcription factors (e.g., AP1, AP3, AG, PI, or SEP3). Consequently, direct interaction of MADS factors AP1, AG, and SEP3 with SYD and BRM ATPase subunits of SWI/SNF complexes (Smaczniak et al., 2012) offers an attractive mechanistic explanation for recruitment of SWI/SNF complexes to these loci. This model is further supported by the observation of Smaczniak et al. (2012) indicating that SWP73B also interacts with the MADS factors AP1, AP3, AG, PI, and SEP3, which are involved in the control of flower development.

Our data demonstrate that SWP73B also plays an important function in leaf development. Inactivation of SWP73B causes very similar leaf developmental defects as the *brm*, *swi3c*, and *swi3d* mutations (Sarnowski et al., 2005; Archacki et al., 2009), which are characterized by a high level of adaxialization leading to downward curvature and twisting. In correlation with the reduced growth rate of abaxial layers, AN3-activated target genes show reduced expression in *swp73b* leaves, supporting the observation that tethering of SWP73B-SWI/SNF complex to AN3 is required for their activation (Vercruyssen et al., 2014). However, the fact that AN3-activated genes show also reduced expression in the *swp73a* mutant, which exhibits normal leaf development, indicates that SWP73B can modulate this pathway independently of AN3. Impaired differentiation of palisade parenchyma and consequent changes in abaxial/adaxial leaf symmetry reflect altered regulation of genes determining leaf polarity in the *swp73b* mutant. Here again, our data show that the *swp73b* mutation causes alteration of nucleosome positioning at important regulatory regions of *AS1*, *AS2*, and *YAB5* promoters, which correspond to known binding sites for GTE6 in the 5′-UTR of *AS1* and KAN1 in the *AS2* promoter. These data are corroborated by detection of cross-linked SWP73 in the same regions by our ChIP-Seq studies. The *AS1* and *AS2* genes

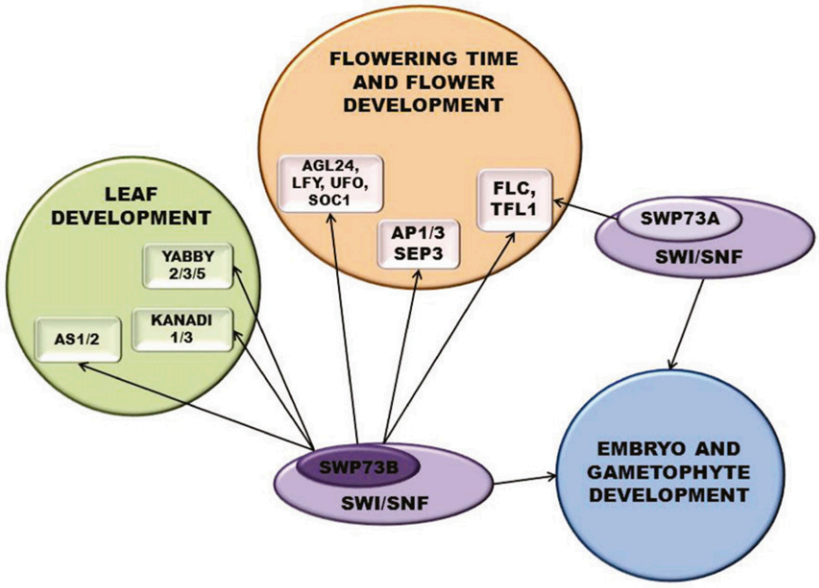

Figure 7. A Model Summarizing Regulatory Functions of SWP73A and SWP73B Containing SWI/SNF Complexes.

specifying adaxial cell fate and *KAN1* determining abaxial polarity are simultaneously derepressed in *swp73b* leaves. Although AS1 and AS2 are coinhibitors of *KAN1*, enhanced *KAN1* expression appears to downregulate other *KAN* and *YAB* genes required for normal cell differentiation in the abaxial layers of *swp73b* leaves. These observations thus suggest that for their transcription repressor functions, both AS1/2 and KAN1 require the recruitment of SWI/SNF complex through SWP73B. In fact, we demonstrated that SWP73B is directly recruited not only to the promoters of *AS1* and *AS2* but also to those of *KAN1*, *KAN3*, *YAB2*, *YAB3*, and *YAB5*. This illustrates that SWP73B plays an important role by directly targeting a set of genes that fine-tune abaxial/adaxial symmetry during leaf development. The distinct and overlapping regulatory roles of SWP73A and SWP73B established in this study are summarized in Figure 7.

METHODS

Plant Lines and Growth Conditions

The *Arabidopsis thaliana swp73a-1 Spm* insertion mutant (SM_3_30546) was identified in the John-Innes transposon mutant collection, whereas T-DNA insertion lines *swp73a-2* (SALK_ 083920), *swp73b-1* (SALK_113834), and *swp73b-2* (SALK_071739) were obtained from the SIGnAL collection of the Nottingham Arabidopsis Stock Centre (Alonso et al., 2003). PCR primers used for genotyping are listed in Supplemental Data Set 2. Seeds were sown on soil or plated on half-strength Murashige and Skoog medium (Sigma-Aldrich) containing 0.5% sucrose and 0.8% agar (pH 5.8). Plants were grown under LD or SD conditions (16 h light/8 h dark or 8 h light/16 h dark, respectively) at 22/19°C, 70% humidity.

Phylogenetic Analysis

ClustalW and MEGA6 software packages were used to align sequences (Supplemental Table 1) and to generate a neighbor joining tree among the SWP73 homologs using 1000 bootstrap replicates (Tamura et al., 2013).

RNA Extraction and qRT-PCR Analysis

RNA was extracted using an RNeasy plant kit (Qiagen) and DNA removed using a TURBO DNA-free kit (Ambion). Total RNA (2.5 μg) was reverse-transcribed using a first-strand cDNA synthesis kit (Roche). qRT-PCR assays were performed with SYBR Green Master mix (Bio-Rad) and specific primers for PCR amplification. qRT-PCR data were recorded and analyzed using iQ-PCR (Bio-Rad) or LightCycler480 (Roche) equipment and software according to the manufacturers. Housekeeping genes *PP2A* and *UBQ5* (AT1G13320 and AT3G62250, respectively) were used as controls. The relative transcript level of each gene was determined by the $2^{-\Delta\Delta Ct}$ method (Schmittgen and Livak, 2008). For each primer pair, the primer efficiency was measured by melting curve analysis. Each experiment was performed using at least two independent biological replicates. qRT-PCR primers are listed in Supplemental Data Set 2.

Production of Genetically Complemented Plants Overexpressing YFP-HA Tagged SWP73B Protein

The *SWP73B* cDNA was cloned into pDONR207, sequenced, and moved into pEarley101 (Earley et al., 2006) using the Gateway procedure. Transgenic lines were generated by floral dip transformation by *Agrobacterium tumefaciens* GV3101 (pMP90) strain carrying *swp73b-1*/+ plants (Zhang et al., 2006) and selected based on their BASTA (100 μM) resistance. Homozygous *swp73b* plants complemented with SWP73B-YFP-HA growing on BASTA-containing medium were identified by PCR-based genotyping.

Yeast Two-Hybrid Assays

The *SWP73A* or *SWP73B* cDNAs were PCR amplified and cloned into the pCR2.1-TOPO-TA vector (Invitrogen), sequenced, and subcloned into the pGBT9 and pGAD424 vectors (Clontech) using *Sma*I/*Sal*I restriction sites. Yeast strain Y190 was transformed with constructs encoding protein pairs to be tested, as well as in combination with either empty pGBT9 or pGAD424 vectors as controls. The expression level of β-galactosidase reporter gene was monitored using the replica filter lift method as described in the Clontech Yeast Protocols handbook.

ChIP

Chromatin was isolated from 2-g samples of 14- or 21-d-old wild-type and *swp73b-1* seedlings and sonicated according to Saleh et al. (2008) with the exception that instead of pepstatin A and aprotinin 1% PIC (Sigma-Aldrich), 1 mM PMSF and 5 mM β-mercaptoethanol were included in the extraction buffer. Cross-linked SWP73B-YFP-HA samples were subjected to immunoprecipitation using 25 μL of GFP-Trap beads (Chromotek) according to the manufacturer's protocol. The percentage of input was calculated using the $2^{-\Delta\Delta Ct}$ method (Schmittgen and Livak, 2008). To facilitate comparison of different samples, the calculated percent input of the wild type was set to 1. The relative enrichment represents the fold change compared with the wild type. The exon region of the retrotransposon gene *Ta3* was used as a negative control (Pastore et al., 2011).

MNase Mapping of Nucleosome Positioning

Mapping nucleosome positioning was performed with 2-g samples of 14-d-old wild-type, *swp73a-1*, and *swp73b-1* seedlings according to Saleh et al. (2008) and Zhu et al. (2013) with minor modifications (i.e., the buffer contained 1% proteinase inhibitor cocktail [Sigma-Aldrich] instead of pepstatin A and aprotinin). Two hundred Kunitz units of micrococcal nuclease (NEB) were used for digestion of each sample. DNA was purified by phenol:chloroform extraction, ethanol precipitation, and size separation on 2% agarose gels. Bands corresponding to ~150 bp were gel isolated, purified, and used for qPCR. Relative nucleosome occupancy was represented as the fraction of undigested chromatin DNA and plotted against the *AP3* gene position with respect to the TSS for each primer pair where the position denotes the center of each 70 to 110 bp amplicon in the *AP3* promoter region.

ChIP-Seq and MNase-Seq

Samples for MNase-Seq and ChIP-Seq were prepared analogously as for MNase and ChIP analyses, respectively, with the exception that 14-d-old seedlings were used. Illumina compatible libraries of MNase-treated genomic DNA were prepared according to the protocol of the Ovation Ultralow DNA Library kit (NuGEN). In contrast to MNase-treated DNA, input DNA was fragmented at first with Covaris S2 to an average size of 200 bp. Libraries were quantified by fluorometry, immobilized and processed onto a flow cell with a cBot (Illumina) followed by sequencing-by-synthesis with TruSeq v3 chemistry on a HiSeq2500.

For MNase-Seq, FastQC (http://www.bioinformatics.babraham.ac.uk/projects/fastqc/) software was used to examine the quality of sequence reads. After trimming using FASTQ Quality Trimmer (Blankenberg et al., 2010), the reads were mapped to the Arabidopsis genome (TAIR10) using BOWTIE2.0 with default settings (Langmead et al., 2009). Nucleosome positioning sequence data were processed by removing clonal reads and extending reads to 150 bp in length using DANPOS (Chen et al., 2013). We

applied quantile normalization methods to occupancy normalization (Wiq function in DANPOS) and Poisson test to differential signal calculation. To identify high-quality nucleosome peaks, the Dpos algorithm was used. To analyze the distribution of a chromatin feature flanking each group of genomic sites (e.g., TSS), we used the Profile algorithm (default settings). Genome-wide distribution of the peak location was visualized using Integrated Genome Browser 8.3.0 (Nicol et al., 2009).

Immunoprecipitated chromatin DNA served as input for Illumina compatible library preparation with the MicroPlex Library Preparation kit (Diagenode). Library output was assessed for quantity by fluorometry (Qubit, Invitrogen) and quality by capillary electrophoresis (Agilent bioanalyzer). Libraries were quantified by fluorometry, immobilized and processed onto a flow cell with a cBot (Illumina) followed by sequencing-by-synthesis with TruSeq v3 chemistry on a HiSeq2500. For ChIP-Seq, FastQC (http://www.bioinformatics.babraham.ac.uk/projects/fastqc/) was used to examine the quality of sequencing reads. After trimming using FASTQ quality trimmer (Blankenberg et al., 2010), the reads were mapped to the Arabidopsis genome (TAIR10) using BOWTIE2.0 with default settings (Langmead et al., 2009). Subsequent analysis indicated the existence of high background in both wild-type and SWP73B samples. Therefore, we employed the analysis according to the advanced SeqMonk manual and decided to use the data for the screen for SWP73B target genes only. Briefly, we applied the extension of reads to 300 bp (as recommended for single-read deep sequencing) and defined probes using MACS peak caller. Subsequently, the P value cutoff 0.05 was applied. The sonicated fragment size was defined as 300 bp and read count quantitation was performed. After application of active probe list peaks, the wild-type value was subtracted from both wild-type and SWP73B-YFP-HA samples and the subtracted data were visualized using Wiggle plot.

Transcript Profiling and GO Study

RNA was isolated from 21-d-old wild-type and *swp73b-1* seedlings using a Plant RNeasy kit (Qiagen) as recommended by the manufacturer. Transcriptomes were analyzed using 150 ng of total RNA as starting material. Targets were prepared with a cDNA synthesis kit followed by biotin labeling with the IVT labeling kit (GeneChip 3′IVT Express; Affymetrix) and hybridized to the ATH1 gene chip for 16 h as recommended by the supplier (gene expression analysis manual; Affymetrix). The raw data were analyzed using GenespringGX (guided workflow) according to the manual. GO analyses of selected groups of genes were performed using GO-TermFinder (Boyle et al., 2004).

In Situ Hybridizations

Methods used for digoxigenin labeling of mRNA probes, tissue preparation, and in situ hybridization were previously described (Bradley et al., 1993) but with small modifications. Instead of Pronase, protease treatment was performed with proteinase K (1 mg/mL in 100 mM Tris, pH 8, and 50 mM EDTA) at 37°C for 30 min. Posthybridization washes were performed in 0.13 SSC (13 SSC is 0.15 M NaCl and 0.015 M sodium citrate). Previously described probes were employed for *AGL24* (Torti et al., 2012) and *AP3* (Zhao et al., 2007). For *AP1*, the template for probes to detect spatial transcript patterns were PCR amplified from cDNA using specific primer pairs (Supplemental Data Set 2) that amplify part of the cDNA with T7 RNA polymerase binding sites attached to the reverse primers.

Microscopic Analyses

Immature seeds were cleared in Hoyer's solution (30 mL of water, 100 g of chloral hydrate, 7.5 g of arabic gum, and 5 mL of glycerin) on a glass slide and examined with a compound microscope equipped with Nomarski optics. For scanning electron microscopy, the plant material was dried in liquid carbon dioxide and mounted on stubs using double-sided adhesive and conductive tabs. Next, plant material was coated with gold and platinum before imaging with a Zeiss Supra 40VP scanning electron microscope (Carl Zeiss NTS).

Alexander Staining

For pollen staining, mature anthers were soaked in Alexander staining solution for 2 h in 50°C in a water bath to detect pollen viability (Alexander, 1969). Stained pollen grains were observed with an Eclipse E-800 microscope. The cytoplasm of a viable pollen grain was stained red purple; the cytoplasm of an aborted pollen grain was green.

BiFC

SWP73B and SWI3D cDNAs were inserted into pDONR207, verified by sequencing, and moved into the pYFN43/pYFC43 vector using the Gateway system. The control vectors (YFN-RFP and YFC-RFP) and the SWI3C-YFC construct were previously described (Sarnowska et al., 2013). Wild tobacco (*Nicotiana benthamiana*) epidermal cells were infiltrated with Agrobacterium GV3101 (pMP90) carrying plasmids encoding SWP73B, SWI3C, or SWI3D fusions and the p19 helper-vector (Voinnet et al., 2003) and analyzed by confocal microscopy 3 d later. In vivo interactions between proteins were detected by BiFC using the Leica TCS SP2 AOBS, a laser scanning confocal microscope (Leica Microsystems). Excitation of YFP was performed with an argon laser line at 514 nm and of RFP with a 563-nm diode laser, and detection of YFP fluorescence was at 518 to 555 nm and of RFP at 568 to 630 nm. The specificity of observed signals was confirmed by measuring the fluorescence emission wavelength (λ scan).

Accession Numbers

Sequence data from this article can be found in the GenBank/EMBL databases under accession numbers *SWP73A* (AT3G01890), *SWP73B* (AT5G14170), *SWI3C* (AT1G21700), and *SWI3D* (AT4G34430) and in the National Center for Biotechnology Information Short Read Archive sequence database (Project ID PRJNA277703). Microarray data are available in the ArrayExpress database (www.ebi.ac.uk/arrayexpress) under accession number E-MTAB-3558.

Supplemental Data

Supplemental Figure 1. Arabidopsis SWP73 Proteins Are Evolutionarily Conserved.

Supplemental Figure 2. Expression Patterns of Arabidopsis *SWP73* Genes Presented in Public Databases.

Supplemental Figure 3. Inactivation of *SWP73B* Gene Causes Severe Developmental Defects.

Supplemental Figure 4. Comparison of Genome-Wide Nucleosome Distribution in Wild-Type, *swp73a-1*, and *swp73b-1* Lines.

Supplemental Figure 5. Transcriptional Profiling of *swp73b-1* Mutant.

Supplemental Figure 6. Genetic Complementation of the *swp73b-1* by the SWP73B-YFP-HA.

Supplemental Figure 7. Analysis of SWP73B-YFP-HA Distribution in the Genome by ChIP-Seq.

Supplemental Figure 8. qRT-PCR Measurement of Transcript Levels AN3 Target Genes in the *swp73b* Mutant and Detailed ChIP-qPCR Mapping of SWP73B in the Promoter Regions of *AS1* and *AS2*.

Supplemental Figure 9. Flowering Time of *swp73a* and *swp73b* Mutants and Detailed SWP73B-YFP-HA ChIP Analysis of the *AP3* Gene.

Supplemental Figure 10. Controls for MNase Protection Assay of the *AP3* Promoter.

Supplemental Figure 11. Ectopic Expression of AP3 in the *swp73b-1* Mutant.

Supplemental Figure 12. SWP73A and *SWP73B* Are Involved in Gametogenesis and Embryogenesis.

Supplemental Data Set 1. Comparative Analysis of Data Sets from MNase-Seq, Transcript Profiling, and ChIP-Seq Analyses.

Supplemental Data Set 2. Primers Used in This Work.

Supplemental File 1. Alignments Used for Generation of SWP73 Phylogeny Tree.

ACKNOWLEDGMENTS

This work was supported by Deutsche Forschungsgemeinschaft Grants KO 1438/13-2 and KO 1438/16-1 to C.K. and A.J., by Ministerstwo Nauki i Szkolnictwa Wyzszego (MNiSW)/National Science Centre Grant N N301 645040 to T.J.S., by Mazovia scholarship 180/ES/ZS-III/W-POKL/14 to S.P.S., and by Diamond Grant NoDI 2011 026941 (MNiSW) to D.M.G. We thank Maida Romera Branchat for providing primer sequences for *AP1* in situ hybridization and Alisdair Fernie for critical comments on the article.

AUTHOR CONTRIBUTIONS

S.P.S. performed research, analyzed data, and wrote the article. D.M.G., E. A.S., P.K., I.J., A.P., E.B., A.T.R., R.F., J.K., K.P., B.H., S.T., and E.S. performed research. E.A.S. and G.C. analyzed the data. A.J. analyzed the data and wrote parts of the article. C.K. analyzed the data and wrote the article. T.J.S. designed the research, analyzed data, and wrote the article.

Received March 17, 2015; revised May 19, 2015; accepted June 3, 2015; published June 23, 2015.

REFERENCES

Albini, S., Coutinho, P., Malecova, B., Giordani, L., Savchenko, A., Forcales, S.V., and Puri, P.L. (2013). Epigenetic reprogramming of human embryonic stem cells into skeletal muscle cells and generation of contractile myospheres. Cell Reports **3:** 661–670.

Alexander, M.P. (1969). Differential staining of aborted and non-aborted pollen. Stain Technol. **44:** 117–122.

Alonso, J.M., et al. (2003). Genome-wide insertional mutagenesis of *Arabidopsis thaliana*. Science **301:** 653–657.

Archacki, R., et al. (2013). BRAHMA ATPase of the SWI/SNF chromatin remodeling complex acts as a positive regulator of gibberellin-mediated responses in Arabidopsis. PLoS ONE **8:** e58588.

Archacki, R., Sarnowski, T.J., Halibart-Puzio, J., Brzeska, K., Buszewicz, D., Prymakowska-Bosak, M., Koncz, C., and Jerzmanowski, A. (2009). Genetic analysis of functional redundancy of BRM ATPase and ATSWI3C subunits of Arabidopsis SWI/SNF chromatin remodelling complexes. Planta **229:** 1281–1292.

Bezhani, S., Winter, C., Hershman, S., Wagner, J.D., Kennedy, J.F., Kwon, C.S., Pfluger, J., Su, Y., and Wagner, D. (2007). Unique, shared, and redundant roles for the Arabidopsis SWI/SNF chromatin remodeling ATPases BRAHMA and SPLAYED. Plant Cell **19:** 403–416.

Blankenberg, D., Gordon, A., Von Kuster, G., Coraor, N., Taylor, J., and Nekrutenko, A.; Galaxy Team (2010). Manipulation of FASTQ data with Galaxy. Bioinformatics **26:** 1783–1785.

Boyle, E.I., Weng, S., Gollub, J., Jin, H., Botstein, D., Cherry, J.M., and Sherlock, G. (2004). GO:TermFinder—open source software for accessing Gene Ontology information and finding significantly enriched Gene Ontology terms associated with a list of genes. Bioinformatics **20:** 3710–3715.

Bradley, D., Carpenter, R., Sommer, H., Hartley, N., and Coen, E. (1993). Complementary floral homeotic phenotypes result from opposite orientations of a transposon at the plena locus of Antirrhinum. Cell **72:** 85–95.

Cairns, B.R., Levinson, R.S., Yamamoto, K.R., and Kornberg, R.D. (1996). Essential role of Swp73p in the function of yeast Swi/Snf complex. Genes Dev. **10:** 2131–2144.

Campi, M., D'Andrea, L., Emiliani, J., and Casati, P. (2012). Participation of chromatin-remodeling proteins in the repair of ultraviolet-B-damaged DNA. Plant Physiol. **158:** 981–995.

Chen, K., Xi, Y., Pan, X., Li, Z., Kaestner, K., Tyler, J., Dent, S., He, X., and Li, W. (2013). DANPOS: dynamic analysis of nucleosome position and occupancy by sequencing. Genome Res. **23:** 341–351.

Chua, Y.L., Channelière, S., Mott, E., and Gray, J.C. (2005). The bromodomain protein GTE6 controls leaf development in Arabidopsis by histone acetylation at ASYMMETRIC LEAVES1. Genes Dev. **19:** 2245–2254.

Crane, Y.M., and Gelvin, S.B. (2007). RNAi-mediated gene silencing reveals involvement of Arabidopsis chromatin-related genes in Agrobacterium-mediated root transformation. Proc. Natl. Acad. Sci. USA **104:** 15156–15161.

Earley, K.W., Haag, J.R., Pontes, O., Opper, K., Juehne, T., Song, K., and Pikaard, C.S. (2006). Gateway-compatible vectors for plant functional genomics and proteomics. Plant J. **45:** 616–629.

Efroni, I., Han, S.K., Kim, H.J., Wu, M.F., Steiner, E., Birnbaum, K.D., Hong, J.C., Eshed, Y., and Wagner, D. (2013). Regulation of leaf maturation by chromatin-mediated modulation of cytokinin responses. Dev. Cell **24:** 438–445.

Euskirchen, G.M., Auerbach, R.K., Davidov, E., Gianoulis, T.A., Zhong, G., Rozowsky, J., Bhardwaj, N., Gerstein, M.B., and Snyder, M. (2011). Diverse roles and interactions of the SWI/SNF chromatin remodeling complex revealed using global approaches. PLoS Genet. **7:** e1002008.

Farrona, S., Hurtado, L., and Reyes, J.C. (2007). A nucleosome interaction module is required for normal function of *Arabidopsis thaliana* BRAHMA. J. Mol. Biol. **373:** 240–250.

Farrona, S., Hurtado, L., March-Díaz, R., Schmitz, R.J., Florencio, F.J., Turck, F., Amasino, R.M., and Reyes, J.C. (2011). Brahma is required for proper expression of the floral repressor FLC in Arabidopsis. PLoS ONE **6:** e17997.

Forcales, S.V., et al. (2012). Signal-dependent incorporation of MyoD-BAF60c into Brg1-based SWI/SNF chromatin-remodelling complex. EMBO J. **31:** 301–316.

Francis, N.J., Saurin, A.J., Shao, Z., and Kingston, R.E. (2001). Reconstitution of a functional core polycomb repressive complex. Mol. Cell **8:** 545–556.

Han, S.K., Sang, Y., Rodrigues, A., Wu, M.F., Rodriguez, P.L., and Wagner, D.; BIOL425 F2010 (2012). The SWI2/SNF2 chromatin remodeling ATPase BRAHMA represses abscisic acid responses in the absence of the stress stimulus in *Arabidopsis.* Plant Cell **24:** 4892–4906.

Hanano, S., and Goto, K. (2011). Arabidopsis TERMINAL FLOWER1 is involved in the regulation of flowering time and inflorescence development through transcriptional repression. Plant Cell **23:** 3172–3184.

Huang, T., Harrar, Y., Lin, C., Reinhart, B., Newell, N.R., Talavera-Rauh, F., Hokin, S.A., Barton, M.K., and Kerstetter, R.A. (2014). Arabidopsis KANADI1 acts as a transcriptional repressor by interacting with a specific cis-element and regulates auxin biosynthesis, transport, and signaling in opposition to HD-ZIPIII factors. Plant Cell **26:** 246–262.

Jack, T., Fox, G.L., and Meyerowitz, E.M. (1994). Arabidopsis homeotic gene APETALA3 ectopic expression: transcriptional and posttranscriptional regulation determine floral organ identity. Cell **76:** 703–716.

Jégu, T., et al. (2013). Multiple functions of Kip-related protein5 connect endoreduplication and cell elongation. Plant Physiol. **161:** 1694–1705.

Jégu, T., Latrasse, D., Delarue, M., Hirt, H., Domenichini, S., Ariel, F., Crespi, M., Bergounioux, C., Raynaud, C., and Benhamed, M. (2014). The BAF60 subunit of the SWI/SNF chromatin-remodeling complex directly controls the formation of a gene loop at FLOWERING LOCUS C in Arabidopsis. Plant Cell **26:** 538–551.

Kumar, S.V., and Wigge, P.A. (2010). H2A.Z-containing nucleosomes mediate the thermosensory response in Arabidopsis. Cell **140:** 136–147.

Lake, R.J., Boetefuer, E.L., Tsai, P.F., Jeong, J., Choi, I., Won, K.J., and Fan, H.Y. (2014). The sequence-specific transcription factor c-Jun targets Cockayne syndrome protein B to regulate transcription and chromatin structure. PLoS Genet. **10:** e1004284.

Langmead, B., Trapnell, C., Pop, M., and Salzberg, S.L. (2009). Ultrafast and memory-efficient alignment of short DNA sequences to the human genome. Genome Biol. **10:** R25.

Lee, J., Oh, M., Park, H., and Lee, I. (2008). SOC1 translocated to the nucleus by interaction with AGL24 directly regulates leafy. Plant J. **55:** 832–843.

Liu, C., Chen, H., Er, H.L., Soo, H.M., Kumar, P.P., Han, J.H., Liou, Y.C., and Yu, H. (2008). Direct interaction of AGL24 and SOC1 integrates flowering signals in Arabidopsis. Development **135:** 1481–1491.

Liu, Z., and Mara, C. (2010). Regulatory mechanisms for floral homeotic gene expression. Semin. Cell Dev. Biol. **21:** 80–86.

Merelo, P., Xie, Y., Brand, L., Ott, F., Weigel, D., Bowman, J.L., Heisler, M.G., and Wenkel, S. (2013). Genome-wide identification of KANADI1 target genes. PLoS ONE **8:** e77341.

Narlikar, G.J., Fan, H.Y., and Kingston, R.E. (2002). Cooperation between complexes that regulate chromatin structure and transcription. Cell **108:** 475–487.

Nicol, J.W., Helt, G.A., Blanchard, S.G., Jr., Raja, A., and Loraine, A.E. (2009). The Integrated Genome Browser: free software for distribution and exploration of genome-scale datasets. Bioinformatics **25:** 2730–2731.

Pastore, J.J., Limpuangthip, A., Yamaguchi, N., Wu, M.F., Sang, Y., Han, S.K., Malaspina, L., Chavdaroff, N., Yamaguchi, A., and Wagner, D. (2011). LATE MERISTEM IDENTITY2 acts together with LEAFY to activate APETALA1. Development **138:** 3189–3198.

Saleh, A., Alvarez-Venegas, R., and Avramova, Z. (2008). An efficient chromatin immunoprecipitation (ChIP) protocol for studying histone modifications in Arabidopsis plants. Nat. Protoc. **3:** 1018–1025.

Sarnowska, E.A., et al. (2013). DELLA-interacting SWI3C core subunit of SWI/SNF chromatin remodeling complex modulates gibberellin responses and hormonal crosstalk in Arabidopsis. Plant Physiol. **163:** 305–317.

Sarnowski, T.J., Swiezewski, S., Pawlikowska, K., Kaczanowski, S., and Jerzmanowski, A. (2002). AtSWI3B, an Arabidopsis homolog of SWI3, a core subunit of yeast Swi/Snf chromatin remodeling complex, interacts with FCA, a regulator of flowering time. Nucleic Acids Res. **30:** 3412–3421.

Sarnowski, T.J., Ríos, G., Jásik, J., Swiezewski, S., Kaczanowski, S., Li, Y., Kwiatkowska, A., Pawlikowska, K., Koźbiał, M., Koźbiał, P., Koncz, C., and Jerzmanowski, A. (2005). SWI3 subunits of putative SWI/SNF chromatin-remodeling complexes play distinct roles during Arabidopsis development. Plant Cell **17:** 2454–2472.

Schmittgen, T.D., and Livak, K.J. (2008). Analyzing real-time PCR data by the comparative C(T) method. Nat. Protoc. **3:** 1101–1108.

Smaczniak, C., et al. (2012). Characterization of MADS-domain transcription factor complexes in Arabidopsis flower development. Proc. Natl. Acad. Sci. USA **109:** 1560–1565.

Strasser, B., Alvarez, M.J., Califano, A., and Cerdán, P.D. (2009). A complementary role for ELF3 and TFL1 in the regulation of flowering time by ambient temperature. Plant J. **58:** 629–640.

Takeuchi, J.K., and Bruneau, B.G. (2009). Directed transdifferentiation of mouse mesoderm to heart tissue by defined factors. Nature **459:** 708–711.

Tamura, K., Stecher, G., Peterson, D., Filipski, A., and Kumar, S. (2013). MEGA6: Molecular Evolutionary Genetics Analysis version 6.0. Mol. Biol. Evol. **30:** 2725–2729.

Tang, X., Hou, A., Babu, M., Nguyen, V., Hurtado, L., Lu, Q., Reyes, J.C., Wang, A., Keller, W.A., Harada, J.J., Tsang, E.W., and Cui, Y. (2008). The Arabidopsis BRAHMA chromatin-remodeling ATPase is involved in repression of seed maturation genes in leaves. Plant Physiol. **147:** 1143–1157.

Tilly, J.J., Allen, D.W., and Jack, T. (1998). The CArG boxes in the promoter of the Arabidopsis floral organ identity gene APETALA3 mediate diverse regulatory effects. Development **125:** 1647–1657.

Torti, S., Fornara, F., Vincent, C., Andrés, F., Nordström, K., Göbel, U., Knoll, D., Schoof, H., and Coupland, G. (2012). Analysis of the Arabidopsis shoot meristem transcriptome during floral transition identifies distinct regulatory patterns and a leucine-rich repeat protein that promotes flowering. Plant Cell **24:** 444–462.

Vercruyssen, L., et al. (2014). ANGUSTIFOLIA3 binds to SWI/SNF chromatin remodeling complexes to regulate transcription during *Arabidopsis* leaf development. Plant Cell **26:** 210–229.

Voinnet, O., Rivas, S., Mestre, P., and Baulcombe, D. (2003). An enhanced transient expression system in plants based on suppression of gene silencing by the p19 protein of tomato bushy stunt virus. Plant J. **33:** 949–956.

Weiner, A., Hughes, A., Yassour, M., Rando, O.J., and Friedman, N. (2010). High-resolution nucleosome mapping reveals transcription-dependent promoter packaging. Genome Res. **20:** 90–100.

Wu, G., Lin, W.C., Huang, T., Poethig, R.S., Springer, P.S., and Kerstetter, R.A. (2008). KANADI1 regulates adaxial-abaxial polarity in Arabidopsis by directly repressing the transcription of ASYMMETRIC LEAVES2. Proc. Natl. Acad. Sci. USA **105:** 16392–16397.

Wu, M.F., Sang, Y., Bezhani, S., Yamaguchi, N., Han, S.K., Li, Z., Su, Y., Slewinski, T.L., and Wagner, D. (2012). SWI2/SNF2 chromatin remodeling ATPases overcome polycomb repression and control floral organ identity with the LEAFY and SEPALLATA3 transcription factors. Proc. Natl. Acad. Sci. USA **109:** 3576–3581.

Zhu, Y., Rowley, M.J., Böhmdorfer, G., and Wierzbicki, A.T. (2013). A SWI/SNF chromatin-remodeling complex acts in noncoding RNA-mediated transcriptional silencing. Mol. Cell **49:** 298–309.

Zhao, L., Kim, Y., Dinh, T.T., and Chen, X. (2007). miR172 regulates stem cell fate and defines the inner boundary of APETALA3 and PISTILLATA expression domain in Arabidopsis floral meristems. Plant J. **51:** 840–849.

Zhang, X., Henriques, R., Lin, S.S., Niu, Q.W., and Chua, N.H. (2006). Agrobacterium-mediated transformation of *Arabidopsis thaliana* using the floral dip method. Nat. Protoc. **1:** 641–646.